ISSN 1173-5996

Modelling Smoke Flow Using Computational Fluid Dynamics

T N Kardos

Supervised by

Dr Charley Fleischmann

Fire Engineering Research Report 96/4
December 1996

This report was presented as a project report
as part of the M.E.(Fire) degree at the University of Canterbury

School of Engineering
University of Canterbury
Private Bag 4800
Christchurch, New Zealand

Phone 643 366-7001
Fax 643 364-2758

Abstract

There have been a number of experimental investigations into the backdraft phenomena. A backdraft occurs in the event of a ventilation source being formed in a compartment, within which a fire has been burning for a sufficiently long enough time to form a deep layer of excess pyrolyzates. The source of fresh air will flow into the compartment in the form of a gravity current. It is the gravity current feature of backdrafts that this research project focuses on.

Application of Computational Fluid Dynamics (CFD) to fire problems is expanding, including the development of specific programs for fire engineering applications. The experimental programme that was used in this research project highlights the difficulties of analysing fluid flows by using CFD simulations. The Flow3D program was used to obtain a more detailed understanding of the behaviour of a gravity current, allowing a detailed study of fluid dynamics which cannot be investigated experimentally. The simulations used two different vent configurations, with the CFD model being validated on the experimental results of salt water tank models. The simulations preformed compared well to the experimental data that was used for scaled salt water tank experiments.

Acknowledgments

There are a number of people who have contributed in some form to this project, and I would like to take this opportunity to thank them.

I wish to thank firstly Associate Professor Andrew Buchannan without whom the Fire Masters programme would not have been. Thanks Andy for all the guidance and support that you have given through out the year.

This work would not have been the same if it was not for my supervisor Dr Charles Fleischmann, who acted as a mentor, adviser and editor. Charley your encouragement and enthusiasm has benefited me immensely, and I shall always remember "Details, Details, Details ..."

Sincere gratitude goes to the New Zealand Fire Service Commission for their finical support for the Masters of Fire Engineering Course. Without their support and devotion to this programme, it would not be as valuable and practical as it has been.

I would like to make a special note of thank you to Tony Enright, who was in last years class, for persuading me to do this course. If it had not been for his enthusiasm it is likely that I would not have enrolled in this course.

Thanks to all my family; Tom, Rosemary and Tillz. Thank you for all your encouragement through my university years and support. A special thanks to dad with your insights during the editing of this.

Thanks to all of the other *fire-boys*; Jason Clement, Mike Radford, Tony Parkes and Michael Belsham. I am sure that the computer room at 3am would not have been the same without your humour and support.

Thank you to Brady Cosgrove, at Works Consultancy Services, for the opportunity to get my feet wet in the fire scene, and to Hamish MacLennan at Holmes Consulting Group, my future employer.

This project would not have been able to get off the ground if it was not for Harwell Laboratories supplying the department an educational copy of Flow3D, and their technical assistance.

A special note of thanks is due to the library staff, who were always able to find the articles that I was after. Even to the point that some would arrive the next day. Without your diligence I am sure that this report would not carry any standing.

I am truly indebted to the cafe ladies, your coffee was a great way to start the day. Thanks also to the computer technical support staff, especially Brandon, without his help I am sure that I would have got lost on an even larger scale in the world of Unix, and X-Windows.

Thank you to all of my friends and flatmates during this period. You all in your own ways helped to keep me sane and freely offered support. Special thanks to AJ and Shane.

Table of Contents

List of Figures and Tables

Nomenclature

A	area (m^2)
C	constant
d	characteristic dimension (m)
g	acceleration due to gravity (m s^{-2})
g'	reduced gravity term (m s^{-2})
H	reference height (m)
h	heat transfer coefficient (kW m^{-1} K^{-1})
I	global coordinates
J	global coordinates
K	global coordinates
k	turbulent kinetic energy
m	mass (kg)
P	pressure (Pa)
$\dot{Q}$	energy release rate (kW)
R	universal gas constant
Re	Reynolds number
S	source or sink term
T	temperature (K)
ΔT	change in temperature (K)
t	time (s)
v	velocity (m s^{-1})
v^*	Froude number
x	horizontal displacement (m)
y	vertical displacement (m)
δ	viscous sub layer thickness (m)
ρ	density (kg m^{-3})
$\Delta\rho$	difference in density between two fluids (kg m^{-3})
μ	viscosity of the fluid (kg m^{-1} s^{-1})
ε	the rate at which turbulent kinetic energy dissipates
ν	kinetic viscosity (m^2 s^{-1})
σ	Stefan-Boltzmann constant 5.67 E-11 (kW m^{-2} K^{-4})
κ	von Karman constant = 0.4
β	normalised density difference (kg m^{-3})
Γ	diffusion coefficient
Φ	fluid characteristic (eg density, pressure ..)

Subscripts

0	ambient fluid
1	original compartment fluid
2	compartment fluid above the gravity current
g	gas
i	i vector
j	j vector
k	k vector

k	effective transfer
O	opening
ref	reference point
T	total of compartment surfaces
t	local
1ε	first energy dissipation term
2ε	second energy dissipation term
*	frictional terms
μ	effect from viscosity
k	effect from turbulent kinetic energy
ε	energy dissipation

1. Introduction

1.1 Purpose of the Research

The purpose of this research was to further investigations into the backdraft phenomena, in particular the gravity current that is the driving force. A backdraft presents a serious hazard to the safety of fire fighters and other personnel attending a fire within a building. The phenomenon arises from a sudden entry of fresh air via a gravity current, into a closed space in which a fire has been burning. This space has accumulated an excess amount of fuel vapour, and with an ignition source results in a deflagration. There have been a number of studies on backdrafts, most of which have used scale models.

Mathematical models for the simulation of fires have mostly been limited to the use of zone models. These divide the compartment into two volumes in which the average properties are calculated as a function of time. While providing useful information, the data from zone models can at best be described as approximations. This project investigates the use of computational fluid dynamics, termed a field model in the fire engineering community, that provides a more accurate prediction than that from a zone model. The computational fluid dynamics model was validated by experiments using a salt water tank model. Although the behaviour of fire is random in nature the use of simulations such as these provides an accurate prediction for the spread of smoke and other toxic substances in the course of a fire.

In the event of a fire in an enclosed room, with little leakage, a hot layer of gaseous combustion products accumulates between the fire and the ceiling. As the fire increases in intensity the available oxygen is consumed and the hot gaseous layer descends, eventually combustion is inhibited. As the fire continues to burn with these limitations, termed a vitiated environment, some of

the fuel can not be burned and will start to accumulate in the gaseous layer. This unburned fuel is known as excess pyrolyzates. If a new ventilation source is introduced, such as a fire fighter opening a door, or a window breaks due to thermal stress, the hot gases within the room flow out of the top of the vent, and the cooler ambient air would flow in at the bottom. The flow of cold ambient air into the room is known as the gravity current[1]. Figure 1-1 shows a sketch of a gravity current when a vent is formed in a previously closed compartment with a fire. The gravity current travels towards the ignition source through the bottom of the vent while hot gases containing excess pyrolyzates exit at the top. In the interface between the gravity current and the layer of hot gases from the leading edge or nose of the gravity current, and the region immediately behind the nose, mixing of the ambient air and excess pyrolyzates occurs. As a result of mixing oxygen and the unburnt fuel, this region will tend to be within the flammable limits. When the gravity current reaches an ignition source the flammable mixture ignites and travels out along the interface of the gravity current and the layer of hot gases. The flow of gases behind the flame front is sufficiently turbulent to increase mixing in this area, this results in combustion in which the flame front travels below the speed of sound, termed turbulent deflagration, within the compartment. This combination of events helps to drive the excess pyrolyzates out of the compartment in an external fireball.

Typically fire fighters that are caught in a backdraft are involved in search and rescue or suppression operations when the explosion occurs. The effects of backdrafts and the terrible consequences that they have on firefighters caught in the path of travel are well documented[2,3,4]. In a recent fire, in March 1994[5], the New York City Fire Department lost three fire fighters after a door was forced open in an apartment building in Manhattan. When the door was opened a large fireball went up the internal stairwell, engulfing the fire fighters on the above landing. This fireball lasted for at least 6½ minutes, killing three men. Although fire service training provides specific warning on backdrafts, in the most reported occurrences the warning signs were not observed in time.

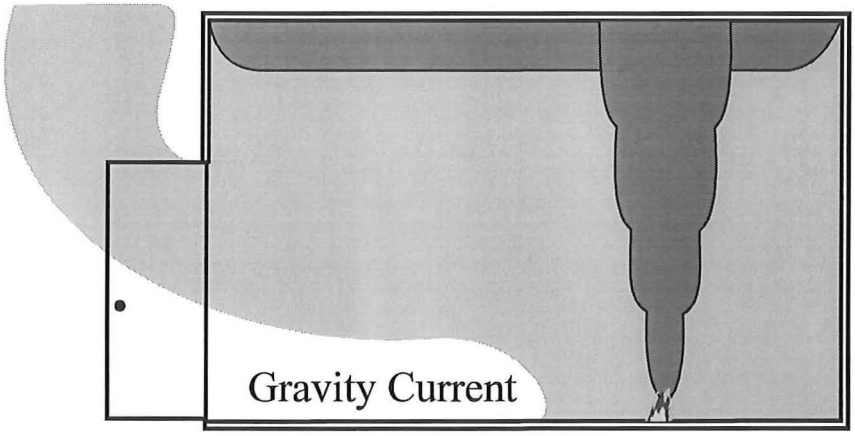

Figure 1-1. Gravity current entering a compartment.

1.2 Zone Model vs Field Model

With a zone model the fire room is considered in two distinct regions of gases, a hot layer at the top and a cooler layer below. The hot layer results from the hot buoyant gases arising from the fire forming a plume. When the plume reaches the ceiling it propagates along the ceiling, then slowly descends filling up the space. The height of this layer is dependent on the presence of openings into the compartment. The two regions of the zone model are treated as internally homogeneous control volumes for which the average properties are calculated by applying fundamental laws and correlations, as a function of time.

Field models on the other hand, break the compartment into many small sub divisions or cells, within which calculations are completed for the conservation of mass, energy and momentum by applying the Navier-Stokes equations. This technique is known as computational fluid dynamics, and the principles have been known for a long period of time. These have been limited in development, due to the time necessary for the calculations in each of the cells. As computing speeds have increased the time taken for these calculations has been reduced, making the developments of computational fluid dynamics models practical.

For most situations that a fire engineer encounters, a zone model would provide an acceptable description of what would happen in the event of a fire. Jassens[6] confirms this, "it is considered that for essentially all fire engineering applications that zone models are more than accurate". The advantage with zone models over computational fluid dynamics is that the calculation times are significantly reduced due to the number of calculations performed.

1.3 Investigation Outline

In 1994 Fleischmann[7] reported on a number of studies into the backdraft phenomena. This work utilised scale experiments to model the phenomena and composed of half scale compartment fires and salt water modelling experiments. Initial experiments lead to a working scenario that these investigations were based.

This work was followed up in 1995 by Bolliger[8], who investigated full size compartment backdrafts. The purpose of this investigation is to continue research into this phenomenon, by applying computational fluid dynamics models to investigate the entering gravity current, which leads up to a backdraft. The investigation is based on the salt water tank simulations of Fleischmann, and uses a number of different vent configurations and different densities of the salt water.

Chapter 2 is a brief discussion on the development of computational fluid dynamics and some interesting quotations on the art of mathematical modelling.

This investigation focuses on the gravity current that leads up to a backdraft and these are discussed in Chapter 3. This incorporates the salt water tank simulations as well as the key features of a gravity current.

The Flow3D computational fluid dynamics package was used and chapter 4 is a summary of the process of applying this software package to model a gravity current. This is extended in Chapter 6 where the final command language and user Fortran files used are discussed in a step by step manner.

Chapter 5 is a review of key articles that have been published in relation to the application of field models in the fire engineering community. A number of different packages have been used, but these all have similarities that they share in common.

The final chapters discuss the results of this investigation and how well the model predicted the behaviour of the gravity current.

1.4 References

[1] Simpson J.E. *Gravity Currents in the Laboratory, Atmosphere, and Ocean*, Annual Review of Fluid Mechanics, Vol 14, 1982, pp 213-234.

[2] *Fatal Mattress Store Fire At Chatham Dockyard*, Fire, 67, 388, 1975.

[3] Russel D. *Seven Fire Fighters Caught in Explosion*, Fire Engineering, April 1983, pp 22-23.

[4] *Backdraft: A Horrible Reality that Kills or Maims in Seconds*, Fire Fighting in Canada, April-May, 1980, pp 4-5.

[5] Bukowski R.W. *Modelling a Backdraft: The Fire at 62 Watts Street*, NFPA Journal, Nov/Dec 1995, pp 85-89.

[6] Jassens M. *Room Fire Models Heat Release in Fires* (Babrauskas V. and Grayson S.J. Editors), Elseiver Science Publishers Ltd, London, 1992, pp 113-157.

[7] Fleischmann C. M. *Backdraft Phenomena*, United States Department of Commerce, National Institute of Standards and Technology, NIST-GCR-94-646, June 1994.

[8] Bolliger I. *Full Residential Scale Backdraft*, Masters Thesis, Department of Civil Engineering, University of Canterbury, Christchurch, New Zealand, 1995.

2. History and Quotations on Modelling

2.1 History and Development of Computational Fluid Dynamics

The ability to accurately predict the behaviour of fires by computational fluid dynamics has resulted from the developments of suitable mathematical methods. These have developed over a period of time.

In 1910, Richardson[1] presented a paper to the Royal Society of London that is considered to be the foundation stone of modern numerical analysis of the partial differential equations, that are necessary for the prediction of fluid flows. In his work, he was able to study differences between steady state and transient flows, and the effects of, sharp corners in the flow field, and boundary conditions approaching infinity. Richardson also investigated the accuracy of numerical methods using Laplacian solutions and was the first to apply these methods on large scale engineering problems, such as the stresses that develop in masonry dams. At that time the calculations were performed by teams of boys, and one of the quickest *computers* averaged about 2,000 Laplacian operations per week, using numbers with only three digits. The main limitation of these computers, was their inability to recognise plus and minus signs.

The method used by Richardson was further improved in 1918 by Leibmann who used only the new terms resulting from the Laplacian operation, to enhance the convergence rate. This simplification had the added bonus of reducing errors in the calculations. Subsequently the focus for computational dynamics was through the use of elliptical equations, as these could be solved by iteration using Leibmann's method. In 1923, Phillips and Wiener[2] improved the convergence rate for this style of iteration, by accounting for the error limits.

In a 1928 publication Courant *et. al.*[3] developed the finite difference method as a mathematical tool. They proved the existence of unique solutions for elliptic, parabolic and hyperbolic systems. The significance of this can be appreciated from three papers published in the IBM Journal in 1967, with the advent of electronic computers, enabling the calculations to be completed with relative ease. Their work forms the basis of the finite difference methods of today.

The first numerical solution to viscous fluid flow was given by Thom[4] in 1933 who extended Leibmann's original method by improving the convergence and error functions. A more efficient method for solving the elliptical equations was developed in 1946 by Southwell[5], called the "Residual Relaxation Method". The advantage of this method of analysis was that a steady state solution could be approached when the difference between iterations is zero.

The first major example of computational fluid dynamics (CFD) was provided by Kopal[6] in 1947, who compiled tables of supersonic flow over sharp cones. This work led to computations being applied to the flight of Intercontinental Ballistic Missiles. The first generation of CFD solutions started to appear in earnest, with the advent of "high speed" computers in the late 1950's. The advances in CFD development can be directly related to advances in computers, most significantly in terms of computational speed and information storage.

In 1966, Moretti and Abbett[7] made a break through, with the development of a time dependant approach to solve the steady state condition. They developed a finite difference solution for blunt bodies at very high velocities and demonstrated the benefits of these, over sharp pointed bodies for atmospheric and high speed travel. Other early pioneers in this field were Fay and Riddell[8] who investigated the stagnation point at high velocities, and Blottner[9] who investigated non-equilibrium boundary layers.

Finite difference solutions have led to manned atmospheric re-entry vehicles for both orbital and lunar missions. The quest for the dominance in space was the principle driving force behind the development of CFD - as only a global race or war situation could.

The power of modern CFD has developed so much that almost all aircraft design tests are completed on a computer, rather than wind tunnel testing. This is partially due the comparative costs, but also because CFD offers the opportunity to obtain detailed flow field information. This may be difficult to measure or is compromised by wall or scale effects in the wind tunnel.

With solutions for the theoretical aspects of fluid dynamics and the availability of high speed computers, race for the development of software packages commenced in the early 1970's. Perhaps one of the best descriptions of this time came from Roache[10].

> ... it is obvious that the general area of computer simulation of physical processes, and the particular area of computational fluid dynamics, is rapidly expanding. One only needs to glance through the titles in any of the scientific abstracting indexes to see the disproportionate number of doctorial dissertations in computational fluid dynamics. Everyone with a computer is computing.

Computational fluid dynamics is still a very active area of research although the focus has changed from writing software to the use of computers to model situations. It is anticipated that in the future there will another change in focus, away from specific research and a few large projects, to a more cost effective method applicable to the design of many smaller projects. In terms of fire safety the current use of zone models will be phased out and replaced with more accurate field models as computers become even more faster and cheaper, and the software becomes cheaper and easier to use.

Although CFD would appear to offer simple solutions to many flow problems, the use of a computer package requires an understanding of the underlying sciences. This is necessary in order to minimise error, as the data processing is only as good as the information entered into the program.

CFD models have been used for the prediction of the spread of fires, in specific projects for almost 20 years. Two recent examples are the investigation into the King's Cross (London) underground station fire in 1987[11], and the design of the English Channel tunnel linking France and England[12].

There are numerous publications that use CFD analysis on compartment fires and there is general agreement amongst them to confirm that CFD models have an acceptable level of accuracy with which the behaviour of fires may be studied.

2.2 Quotes on Modeling

Some interesting quotations come from Leendertse[13] who describes the art of modelling.

> This is the problem: the process by which a model in general is derived at can at best be described as an intuitive art, and creativity of the modeller is *the* important ingredient for a successful model investigation; creativity cannot be replaced by scientific knowledge.
>
> Modeling is certainly not a scientific endeavour, even though it is customary to report it as such. Successful modeling is nearly always reported as a more or less logical reconstruction of occurrences. Derivations are presented in a logical sequence which has little relationship to the manner in which modeling effort progressed. Generally many attempts were made to produce results and only the finally chosen was reported.
>
> The reason why we do this is that the modeller wants to make their work acceptable to the scientific community. Also, it provides a convenient, acceptable frame for reporting. As a result an unrealistic

> view is presented as to what modelling actually is and how it is done.

This is furthered with a later quote.

> The way in which a modeller derives a model for the system he is studying can be best described as an intuitive art. No fixed rule can be given. The modeller must have the ability to analyse the problem, abstract the *essential* features, select and modify assumptions that characterise the system, and subsequently extend and enrich it until a useful approximations is found...Moreover,...the modeller is at least as important as the model which is used.

2.3 References

[1] Richardson L.F. *The Approximate Arithmetical Solution of Finite Differences of Physical Problems Involving Differential Equations, with an Application to the Stresses in a Masonry Dam*, Transactions of the Royal Society of London, Ser A, Vol 210, 1910, pp 307-357.

[2] Phillips H. and Wiener N. *Nets and the Dirichlet Program*, Journal of Mathematics and Physics, Vol 2, 1923, pp 105-124.

[3] Courant R. Friedrichs K.O. and Lewy H. *Uber die Partiellen Differenzengleichurgen der Mathematischen Physik*, Mathematische Annalen, Vol 100, 1928, pp 32-74.

[4] Thom A. *The Flow Past Circular Cylinders at Low Speeds*, Proceedings of the Royal Society of London, A141, 1933, pp 651-666.

[5] Southwell R.V. *Relaxation Methods in Theoretical Physics*, Oxford University Press, New York, New York, 1946.

[6] Kopal Z. *Tables of Supersonic Flow Around Cones*, Department of Electrical Engineering, Centre of Analysis, Massachusetts Institute of Technology, Cambridge, 1947.

[7]Moretti G. and Abbett M. *A Time Dependent Computational Method for Blunt Body Flows*, AIAA Journal, Vol 4, No 12, December 1966, pp 2136-2141.

[8] Fay J.A. and Riddell F. R. *Theory of Stagnation Point Heat Transfer in Dissociated Air*, Journal of the Aeronautical Sciences, Vol 25, No 2, February 1958, pp 73-85.

[9] Blottner F.G. *Non-equilibrium Laminar Boundary-Layer Flow of Ionised Air*, AIAA Journal, Vol 2, No. 11, November 1964, pp 1921-1927.

[10] Roache P. J. *Computational Fluid Dynamics*, Hermosa Publishers, Albuquerque, 1972.

[11] Simcox S., Wilkes N.S. and Jones I.P. *Computer Simulation of the Flows of Hot Gases from the Fire at King's Cross Underground Station*, Fire Safety Journal, Vol 18, 1992, pp 49-73.

[12] Kumar S. *Field Model Simulations of Vehicle Fires in a Channel Tunnel Shuttle Wagon*, Fire Safety Science Proceedings of the Fourth International Symposium, 1994, pp 995-1006.

[13] Leendertse J.J. (Discussion in,) *Transient Models for Inland Coastal Waters* (by H.B. Fisher), Academic Press, 1981.

3. Literature Review

3.1 Introduction

There have been many publications that describe of the use of field models for predicting the behaviour of fires, in different situations, and under different conditions. A comprehensive review of all the literature is beyond the scope of this thesis. However key field modelling reports of specific relevance to this investigation are summarised in this section.

3.2 Papers Using Flow3D

Flow3D is one of a number commercially available CFD software packages. It has been used to model a variety of fire simulations and since its introduction has been upgraded several times to become more comprehensive, facilitate ease of operator use and improve graphic presentation of results.

3.2.1 A Comparison of a FLOW3D Based Fire Field Model with Experimental Room Fire Data[1]

Kerrison *et. al.* conducted a series of trials in order to compare the predictions of Flow3D with experimental data obtained for small room fires. They used a 2.8m square room with a 2.18m high ceiling and a single vent, a door. Their heat source was a methane burner that was moved around the room to various locations. The burner was not modelled using a combustion algorithm, but instead the calculated heat produced from the burner, reduced to account for the loss of radiation to the walls was used. Turbulence was modelled using the standard k-ε algorithm with a buoyant, compressible flow. Solution algorithms comprised of the Hybrid differencing scheme, and Stone for momentum and enthalpy. The grid was extended out through the door, so that the flow through

the vent could be modelled. Boundary conditions were based on the ambient with the walls treated as non-slip surfaces.

With fires located in the centre of the room the results obtained for the temperature and heat flux for the upper layer, were consistent with the measured experimental data. In the case of the walls being adiabatic the predictions showed deviations from the experimental results. With the burner located near a wall the predictions of the model showed deviations of over 20% for the upper layer temperature and 40% for heat flux.

These results suggest that for similar situations the model parameters should incorporate non-adiabatic boundary conditions with a centred room fire.

3.2.2 Computer Simulation of the Flows of Hot Gases from the Fire at King's Cross Underground Station[2]

The King's Cross (London) underground fire spread much more quickly than was anticipated. During the post-fire investigation Simcox *et. al.,* the authors of this paper, were approached to simulate the course of the fire using a field model. As a result of the predictions derived for this fire the *'trench effect'*, was described.

The model used the Hybrid differencing scheme and SIMPLEC for non-linear coupling equations, Stone for velocity and the ICCG for pressure correction. Turbulence was modelled using the k-ε model with a buoyant flow. Initially an incompressible flow was used, and thereby calculations were carried out using the Boussinesq approximation. The flow was later modified to be fully compressible. Combustion was not modelled, again to simplify the model, instead a time-varying heat source was used that ignored the effects of radiation. All vents were described as pressure boundaries, and the grid terminated at these boundaries. This resulted in some of the gases being sucked out of the stream in the upper layer, and being drawn in near the bottom layer. This effect is known

to occur during the course of a fire but the prediction from the model was an order of magnitude greater than expected.

The results obtained from of the model were consistent with the pattern of fire spread reconstructed from scorch marks and smoke damage during the investigation. The inquiry into this fire used information based on this model along with additional experiments to explain the fire's spread. This report demonstrates the ability of field models to show detailed flow analysis when they are accurately applied.

3.2.3 Field Modelling: Effects of Flat Beamed Ceilings on Detector and Sprinkler Response[3]

Prediction on the spread of fire and smoke, and early detection forms an integral part of building safety. This group of authors are using field models with the aim to improve the building code requirements for the location of sprinklers and heat detectors. This is the first year report of a four year project, in which predictions of fires in rooms with flat ceilings and exposed beams have been published.

Combustion was not modelled as it was decided that the lack of radiation sub-models would contribute a significant source of error. Heat was modelled at a specific point with varying intensity. Turbulence was modelled with the standard k-ε model, and the flow was fully compressible. Their intention was to investigate the dependence on compressibility by using either the Boussinesq approximation or by neglecting the pressure wave propagation, but little was published on these results. The walls were fully insulated and were assumed to be adiabatic. As these would reach the gas temperature quickly and there would be little heat loss. The Upwind differencing scheme was used with a non-slip boundary condition on the walls. Wood cribs were burned in the experiments and the heat release rate was calculated with an allowance of 35% heat loss by radiation and was used in the simulation.

The predictions of the model and experimental data for fire temperature did not always coincide. The authors thought that this discrepancy is most likely to be due to the lack of terms to adequately describe the effects of radiation. For many of the other parameters the predictions were consistent with much of the experimental data, included the hot gases being channelled from one beam to another and the sensor activation times.

3.2.4 Field Modelling: Simulating the Effect of Sloped Beamed Ceilings on Detector and Sprinkler Response[4]

This is the second year report from the above group, and it extends their original report using the standard k-ε model. With low ceilings, there was no significant advantage in making the modification suggested by Nam and Bill[7]. All surfaces were treated as adiabatic, but this was found to be a major source of error especially when the beams were running perpendicular to the ceiling slope. The error was due to the hot gases remaining in contact with the ceiling for longer than anticipated hence some heat was lost through the ceiling. The experimental data and model predictions showed that the detector response time was not affected by the adiabatic assumption.

3.2.5 Field Modelling of Room Fires[5]

In this report single and three room compartment fires were modelled for temperature predictions, and compared to experimental data. The fire was modelled as a heat source based on the experimentally measured heat release rate, allowing for a 35% loss due to radiation.

The model used the k-ε turbulence formulae, with fully compressible air as the working fluid. The walls were treated as adiabatic surfaces except for one case in the analyses of the three rooms, where the ceiling was set as being conductive. Two dimensions were used and the effects of varying the vent boundary conditions were also studied. This was achieved by defining the vent as a pressure boundary, representing the atmosphere or using another space as the ambient conditions. It was noted that there was a small difference for

temperature between the model and the experimental burn, except for just inside the vent where the temperature predicted by the model was underestimated by 10%. The results of this study showed that valid predictions could only be obtained for a direct opening vent when the heat source is a significant distance away from the vent.

The fire was modelled as a constant volume (one cell) but with a varying heat release rate. During the experimental burn there were a number of fusible links placed on an instrument tree and these were modelled for activation time within the model by using the algorithm from LAVENT.

The comparison between prediction and actual burn were favourable, and the activation times for the links obtained by LAVENT closely correlated in the case of the single room fire. It was noted that if the layer height was fixed at a lower level in the model, there was minimal difference between the predicted and actual activation times. It was also noted that by increasing the number of inner iterations, from 20 to 50 for the pressure term, there was a 3rd order of magnitude reduction in the mass residuals. This significantly improved the computational efficiency by increasing the rate of convergence.

In the case of the three rooms, the space was modelled in three dimensions, and consisted of two rooms linked together by a long corridor. There was reasonable consistency between the predictions of the model and the experimental data for temperature, however temperatures near the floor and ceiling were greater than those predicted. This error is thought by the authors to be due to the lack of radiative heat in these areas. Otherwise the temperature predictions were consistent, in the room with the fire, but less accurate in the other rooms. This inaccuracy may have been due to grid dependence, or due to the lack of conductive heat transfer to the walls.

3.3 Phoenics

Phoenics is another commercially available CFD package, written as a combustion model. It has wide acceptance as a field model in the fire engineering community.

3.3.1 A Critical Comparison of a Phoenics Based Fire Field Model with Experimental Compartment Fire Data[6]

In this paper the authors describe a model that is very similar to that (section 5.2.1) for Flow3D. The space was a 2.8m square room with a 2.18m high ceiling and a single vent. The heat source was provided by a methane burner, which was moved around the room to various locations. The model used the effective heat output allowing for radiative losses. Turbulence was modelled with the k-ε scheme with modifications for buoyancy terms.

As was the case with Flow3D, comparisons between the predictions and the experimental data were good when the heat source was away from the walls, but when the heat source was adjacent to a wall there was an under prediction of 20% in mass flux. This was assumed to be due to the effect of radiative transfer to the wall being significant. The authors thought that this could possibly be accounted for if the model was to include the effects of combustion. With a methane fire the products of combustion have negligible effect on radiation so the lack of combustion radiation modelling would seem to be a reasonable approximation. In the upper layer temperature there is an over prediction of 11% for the centred fire and this extends to over +44% at the wall location.

3.3.2 Numerical Simulation of Thermal Plumes[7]

In this paper thermal plumes were generated from a heptane spray fire and these are compared to the Phoenics field model. This research investigated the effect of altering the k-ε algorithm so that it no longer over predicted temperature and velocity along the center-line of large buoyant plumes. Although the Algebraic

Stress Model (ASM) works well in this situation, it has the disadvantage in that it requires significantly more computational time. The fires were modelled as a cylinder of flame that varied in height and radius.

It was suggested by the authors that the turbulent viscosity (C_μ) be increased to 0.18, from 0.09 and lower the effective Prantl number (σ_k) to 0.85, from 1.0 in order to obtain a better prediction for large buoyant plumes. It was noted that there was less than 2% discrepancy with this modification, compared to over 60% for temperature and 25% for velocity with the unmodified model.

3.4 Jasmine

Jasmine is based on the Phonics code but it is fire engineering specific. A number of investigations have been performed with this program with mixed results.

3.4.1 Modelling the NIST High Bay Fire Experiment with Jasmine[8]

The aim of this research was to determine the accuracy of Jasmine for modelling atria and other large open space areas such as what would be found in shopping malls. In the experimental situation the ceiling consisted of a number of exposed 'I' beams that channel the smoke flow.

The model was based on an alcohol pool fire, ignoring the effect of radiation. There is little information supplied in this paper about the model set up, however the authors suggest that the model compared well to experimental data. With the upper layer temperature the error ranged from ±5°C to ±17°C, however allowing for a ±2.5°C error in the experimental data the predictions may in fact be better.

3.4.2 Computational Field Models in Fire Research and Engineering[9]

The author of this paper, Bilger, is committed to the development of field models in the fire engineering community instead of using traditional zone models. With modelling buoyant flows it was noted that the current state of knowledge is far from satisfactory, and that turbulent fire plumes may not be well modelled with the k-ε method. Instead a second order closure model, such as the ASM, may be necessary, but there is trade off between computational time and validity of predictions. The ASM is computationally more intensive, so it is worthwhile to try to improve the k-ε model. It is noted that the ASM model is currently used for modelling most meteorological flows. Another problem with the k-ε model is that it unsatisfactorily models heat transfer at the stagnation point. Again this is modelled better with the ASM, and it is noted although the k-ε gives the correct answer, this could be for the wrong reason.

Other key areas that the reader is drawn to with field modelling of combustion is that;

- with validation of a fire with alcohol or natural gas as the fuel, no soot will be produced, therefore there will be no radiation losses, quenching, and products of combustion such as C, CO or unburnt hydrocarbons in the plume,
- the field models do not allow for the pyrolysis of the neighbouring fuels,
- there is no accounting for the condensation of species such as tar.

Bilger suggested that with the current lacking of understanding of applying field models, there needs to be developed a hierarchy of well documented and well-vetted experimental data on buoyant flows and fires upon which future field models can be based. In the design of field models there is always the human element, with the likelihood of human error resulting. An applicable quotation is; "Erroneous treatment of sub-models can result in no error at all."

3.5 Other Field Models

3.5.1 Fire Computation: The 'Flashover' Phenomenon[10]

This paper describes an in-house field model written at the Imperial College, and investigates the predicability of flashover, based on heat transfer to the surroundings from the fire. The k-ε turbulence model is used, and results are compared to experimental data.

For both computational stability and improved convergence the boundary conditions include extension of the computational space out of the compartment into the ambient, with the remaining conditions atmospheric. The walls were assumed to conduct some of the heat away, and the effect of soot on radiation was modelled using a simple kinetic expression.

The model agrees with reasonable accuracy, allowing for some scatter, to within 20% for the central temperatures but was not quite so accurate for the surface temperatures of the walls.

3.5.2 Gravity-Current Transport in Building Fires[11]

This paper is a summary of the effects of a gravity current in transporting the products of combustion and the key features involved in modelling one, using a field model.

The flow was assumed to be incompressible and thereby the authors applied the Boussinesq approximation. Turbulence was modelled by using a second order closure model, the ASM, with mixing playing an important role. The calculations were based upon the walls remaining cool allowing for heat transfer.

Gravity currents are three dimensional in nature, however these studies have shown that their large scale effects can be modelled in two dimensions, with reasonable agreement between experimental data and model predictions.

3.5.3 Mathematical Modelling of Buoyancy-Induced Smoke Flow in Enclosures[12]

This is a two-dimensional model that investigated the non-uniform buoyant forces that effect the flow. The model space extended through the vent. The Upwind difference scheme and the k-ε turbulence model, modified for use with elliptical flows were used. The Boussinesq approximation was made, and the walls were treated as non-slip surfaces with a logarithmic profile near the surface. The boundaries were adiabatic, and the fire heat release rate was based on a methylated spirits pool fire.

The model over-predicted the hot layer depth. This was especially notable at the opening. It is noted that the k-ε model, although adequate, may not be the best choice.

3.5.4 Simulation of Airflow Through Large Openings in Buildings[13]

This paper investigated simulation of a gravity current in a large building by using a heater as the heat source with an opening to the ambient conditions. Particular emphasis was placed on the flow field rather than wall effects and heat transfer. The computational grid was also extended through an opening to improve computational accuracy. The model predictions were compared to simple hand calculations such as Bernoulli's equations.

The field model used a k-ε algorithm for turbulence, applying the Upwind differencing scheme with an incompressible fluid, and therefore the Boussinesq approximation was used. The walls were treated as having a logarithmic profile near the wall for the velocity profile in the boundary layer, and all surfaces were treated as being adiabatic.

The predicted values of peak temperature, velocity and the velocity profile correlated very well (less than 2%) in two dimensions. With the addition of the effect of wind, it turned out that there was less than 10% difference between the forced convection and the free convection flows, with the forced flow being smaller.

3.6 References

[1] Kerrison L. Galea E.R. Hoffman N. and Patel M.K. *A Comparison of a FLOW3D Based Fire Field Model with Experimental Room Fire Data*, Fire Safety Journal, Vol 23, No 4, 1994, pp 387-411.

[2] Simcox S., Wilkes N.S. and Jones I.P. *Computer Simulation of the Flows of Hot Gases from the Fire at King's Cross Underground Station*, Fire Safety Journal, Vol 18, 1992, pp 49-73.

[3] Forney G.P. Bukowski R.W. and Davis W.D. *Field Modelling: Effects of Flat Beamed Ceilings on Detector and Sprinkler Response*, National Fire Protection Research Foundation, 1993.

[4] Davis W.D. Forney G.P. and Bukowski R.W. *Field Modelling: Simulating the Effect of Sloped Beamed Ceilings on Detector and Sprinkler Response*, International Fire Detection Research Project, National Fire Protection Research Foundation, 1994.

[5] Davis W.D. Forney G.P. and Klote J.H. *Field Modelling of Room Fires*, United States Department of Commerce, National Institute of Standards and Technology, NISTIR 4673, 1991.

[6] Mawhinney R.N. Galea E.R. Hoffmann N. and Patel M.K. *A Critical Comparison of a Phoenics Based Fire Field Model with Experimental Compartment Data*, Journal of Fire Protection Engineering, Vol 6, No 4, 1994, pp 137-152.

[7] Nam S. and Bill R.G. *Numerical Simulation of Thermal Plumes*, Fire Safety Journal, Vol 21, 1993, pp 231-256.

[8] Tubbs J.S. and Barnett J. *Modelling the NIST High Bay Fire Experiment with Jasmine*, Proceedings of the International Conference on Fire Research and Engineering, 1995, pp 383-388.

[9] Bilger R.W. *Computational Field Models in Fire Research and Engineering*, Fire Safety Science Proceedings of the Fourth International Symposium, 1994, pp 95-110.

[10] Lockwood F.C. and Malalasekera W.M.G. *Fire Computation: The 'Flashover' Phenomenon*, Twenty-Second Symposium (International) on Combustion, The Combustion Institute, 1988, pp 1319-1328.

[11] Baum H.R., Cassel K.W., McGrattan K.B. and Rehm R.G. *Gravity-Current Transport in Building Fires*, Proceedings International Conference on Fire Research and Engineering, 1995, pp 27-32.

[12] Markatos N.C. Malin M.R. and Cox G. *Mathematical Modelling of Buoyancy Induced Smoke Flow in Enclosures*, International Journal of Heat and Mass Transfer, Vol 25, No 1, 1982, pp 63-75.

[13] Schaelin A., van der Maas J. and Moser A. *Simulation of Airflow Through Large Openings in Buildings*, ASHRAE Transactions: Symposia, Vol 98, part 2, 1992, pp 319-328.

4. Modelling Gravity Currents

4.1 Introduction

This section reviews key features that need to be considered in modelling gravity currents when using CFD. In order to model a gravity current it is necessary to have an understanding of its behaviour. When a gravity current enters a compartment during a fire it consists of fresh air that is mixed with the fuel vapour in the compartment. This mixing arises due to the turbulent nature of the current. Turbulence modelling is a developing science and the choice of turbulence scheme and the parameters used to describe this turbulent mixing of the hot and cold gases is important in determining the outcome. In order to validate the prediction of the CFD model developed, results were compared to the salt water tank simulations completed by Fleischmann[1].

4.2 Gravity Currents

Gravity currents arise from the buoyant forces due to density variations in the fluids, subject to gravitational force. Gravity currents occur in nature in many different forms. Perhaps the most common example of a buoyancy driven gravity current is a sea breeze. In which during the day there is a cool breeze from the sea to land, and at night a warm breeze with the direction reversed. There are many other examples of gravity currents which are evident in every day life these include;

- dust storms
- weather fronts
- fog banks
- avalanches, due to suspended particles
- a cold draft through the house
- mixing of salt and fresh water at a river mouth
- oil slicks

With two fluids, either liquid or gaseous, of differing density, the lighter fluid will flow over the top of the heavier fluid, forming a gravity current. What happens is very similar to having a door open on a cold day, the hot less dense air escapes at ceiling level and cooler more dense air enters at floor level.

In the event of a fire in a building, there will be gases at different temperatures and therefore differing densities. The resulting gravity current can transport smoke, hot gases and other toxic substances present, through out the building. This is particularly relevant in buildings with long corridors linking adjoining rooms, as this path of travel will be quickly engulfed, rendering it untenable.

In the event of a fire in a compartment, figure 4-1, with limited ventilation, the fire continues to grow until there is insufficient oxygen to sustain complete combustion of the fuel. At this time the fire is sufficiently large enough to continue the pyrolysis of the solid fuel. These pyrolyzates will have insufficient oxygen to react with and will accumulate in the hot gas layer, figure 4-2.

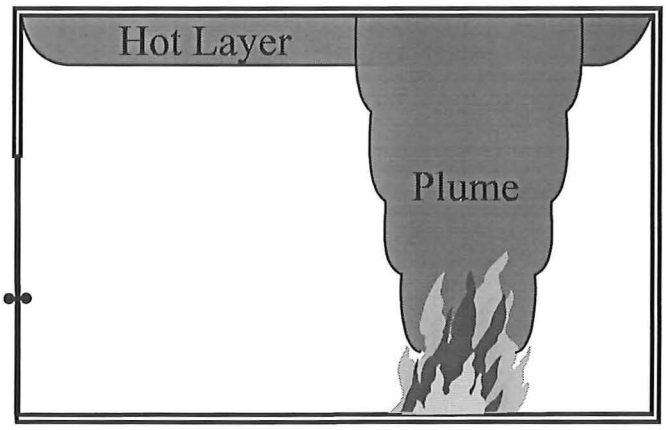

Figure 4-1. Fire Development closed compartment.

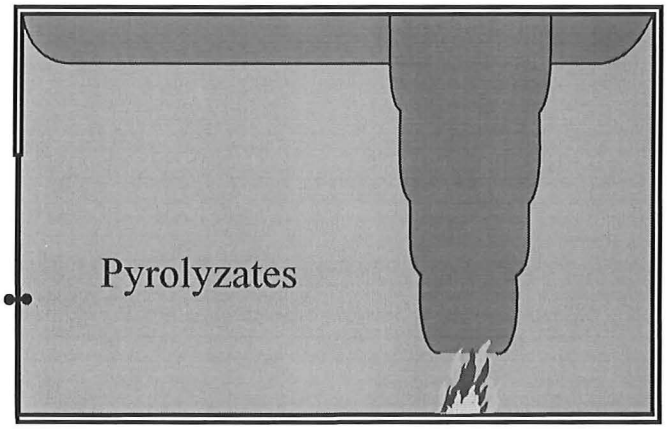

Figure 4-2. Excess pyrolyzates due to lack of air.

Supposing a new ventilation source suddenly becomes available, as would happen if someone was to open a door, or a window was to shatter due to thermal stress, the hot gas layer will move out of the compartment at the top of the vent. Fresh air will enter at the bottom of the vent to replace the volume of gas that has escaped as a gravity current, figure 4-3. The entering air will mix in the compartment with the fuel rich gases, and on reaching an ignition source there will a suitable air fuel mixture to bring about complete combustion. This will culminate in a deflagration within the compartment and resulting in the phenomena known as a backdraft, eventuating with an external fireball.

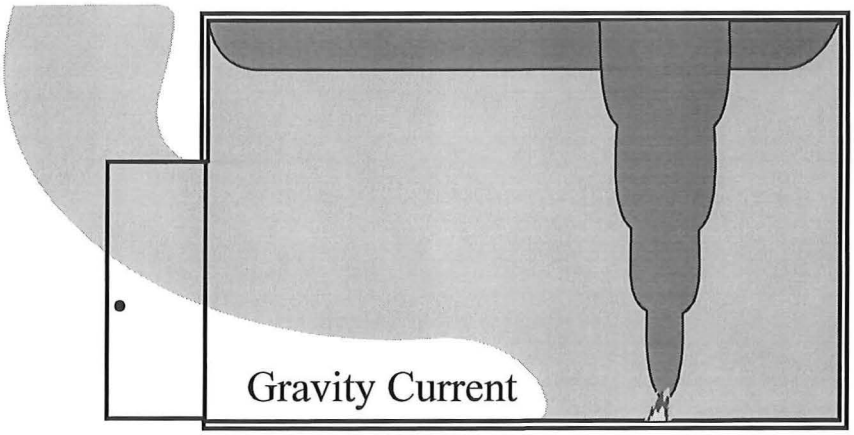

Figure 4-3. Incoming gravity current.

The key steps of a backdraft are therefore;

- the accumulation of unburnt gaseous fuel,
- an oxygen rich gravity current which mixes with the fuel rich compartment gases,
- ignition of the mixed gases,
- turbulent deflagration.

A gravity current has many attributes, one of the simplest descriptions comes from Simpson[2], with a dam-break analogy. Consider a full hydro dam, and all of a sudden it develops a hole. Initially there will be a horizontal jet of water on which gravity will act, causing the flow to become vertical. The loss of potential energy results in a gain of kinetic energy, along with frictional losses and viscous heating of the fluid consistent with the laws of conservation of energy. These latter two terms will tend to be minimal.

Therefore from the conservation of energy the behaviour of the gravity current can be expressed mathematically as,

$$\frac{mv^2}{2} = mg\frac{H}{2} \qquad \text{Equation 4-1}$$

which simplifies to,

$$v = \sqrt{gH} \qquad \text{Equation 4-2}$$

or with two different fluids,

$$v = \sqrt{\frac{\Delta\rho}{\rho} gH} \qquad \text{Equation 4-3}$$

where $\Delta\rho$ is the density difference of the two fluids, and ρ is the density of the less dense fluid.

The fluids involved in a gravity current may be chemically different but the driving force is due to differences in their density, arising from either the presence of dissolved material or differences in temperature.

The dependence on Reynolds number for the shape leading nose of the gravity current has been known since 1911 by the work of Schmidt[3].

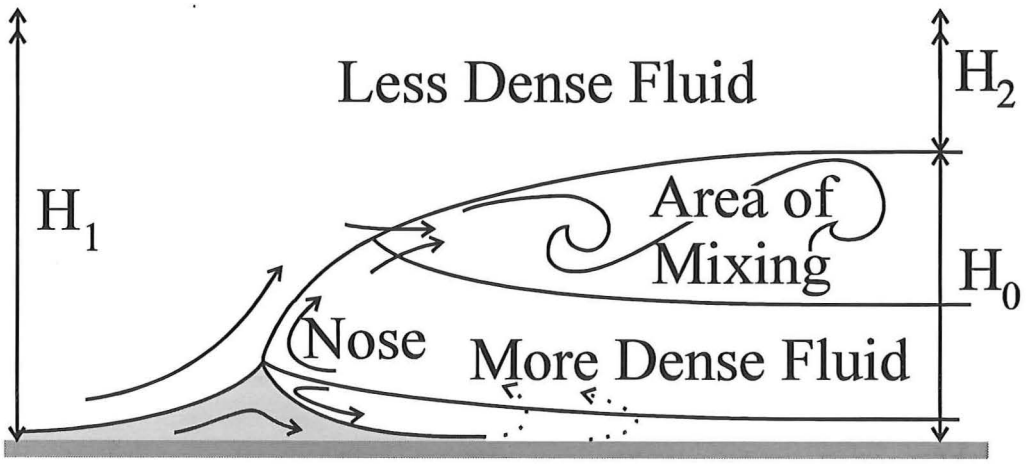

Figure 4-4 Sketch showing the key features of a gravity current adapted from Simpson[1].

It can also be shown that the fractional depth, $\frac{H_0}{H_1}$ plays an important role with the Froude number, $v^* = \frac{v}{\sqrt{g' H_0}}$ where g′ is the reduced gravity term and $g' = g\frac{\Delta\rho}{\rho}$.

When both buoyancy and momentum are of equal importance, the non-dimensional Froude number is used to quantify their relative magnitudes. For example, a high velocity in a small opening would have a high Froude number, but if the opening was made larger the Froude number would be less.

Most gravity currents will have turbulent mixing at the front but not in all cases, for example an oil slick. Turbulent mixing plays an important role in the dynamics of the flow, as the mixing region has both non-uniform velocity and concentration profiles.

Figure 4-4 shows the flow pattern with the foremost point raised from the surface. This is due to friction over a non-slip boundary, ie the velocity of the flow at the wall is zero, that explains the lifting off, and tucking under, allowing of some of the ambient fluid to pass underneath the gravity current.

4.3 Turbulence

Turbulence is an irregular condition in which, for example velocity, pressure, concentration, and temperature, vary randomly in time and space for a fluid flow. The motion is always rotational with large eddies effected by the boundary conditions, and small eddies effected by the internal viscous forces. The general definition for turbulence is a high Reynolds number, $Re \equiv \frac{\rho v d}{\mu}$. The approximate flow regime for a flow in a duct is;

Laminar Flow	$Re < 2{,}000$
Transition	$2{,}000 < Re < 4{,}000$
Turbulent	$Re > 4{,}000$

This regime for turbulence has needed to change with CFD programs becoming more powerful and capable of resolving the flow field. A more appropriate definition with the use of computers would be where the fluid flow is not resolvable with the user's grid. This means that with a fine enough grid, the flow may not be turbulent.

Fluid flows in a room fire will generally be turbulent, with vortices of varying size and frequency. These vortices will get smaller with time as the flow starts to settle, eventually reaching a size where the viscous forces dominate and the vortices break-up. In order to model the behaviour of the vortices during a turbulent flow, the grid used by the CFD program would have to be very small, in the order of a less than a millimetre. Such a small size would require a very large computational space, and would be time consuming. So with the limitations of computational power it is necessary to compute the effects of turbulence through alternative means. These are known as *sub grid* models, in which the flow equations are averaged over both time and space.

All turbulence models are approximations based on the assumption that with a fine enough scale ie a very small grid, all turbulent flows obey the Navier-Stokes equations.

The four main classifications of sub grid models are;

Classical Based on (time averaged) Reynolds Equations

Eddy viscosity
1. zero equation model - mixing length model
2. two equation model - $k-\varepsilon$ model

Second order closure
3. Reynolds stress equation
4. Algebraic stress method

Large eddy simulation Based on space - filtered equations

Flow3D solves the sub grid equations in methods 2, 3, and 4 of the above.

The mixing length model describes the transport of the flow by simple algebra as a function of position, while the k-ε model accounts for the transport of the turbulence parameters within space and time. The Reynolds stress algorithm uses partial differential equations of the unknown terms, based on the transport equations for the dissipation of turbulent kinetic energy. The algebraic stress method is formed by simultaneously solving the k-ε and Reynolds stress models.

The idea of using transport equations to describe the movement of the physical properties of a flow has been around since the early 1920's. A key step forward came in the 1940's with Kolmogorov[4] and Prantl[5], who independently showed that eddy viscosity is dependant on a direct proportionality.

The model transport equations of the standard k-ε model can be simply represented by the following, where k is the turbulent kinetic energy, and ε is the rate at which this energy dissipates;

$$\begin{bmatrix}\text{Rate of}\\ \text{change of}\\ k \text{ or } \varepsilon\end{bmatrix} + \begin{bmatrix}\text{Transport}\\ \text{of } k \text{ or } \varepsilon \text{ by}\\ \text{convection}\end{bmatrix} = \begin{bmatrix}\text{Transport}\\ \text{of } k \text{ or } \varepsilon \text{ by}\\ \text{diffusion}\end{bmatrix} + \begin{bmatrix}\text{Rate of}\\ \text{production}\\ \text{of } k \text{ or } \varepsilon\end{bmatrix} - \begin{bmatrix}\text{Rate of}\\ \text{destruction}\\ \text{of } k \text{ or } \varepsilon\end{bmatrix}$$

Equation 4-4

or algebraically,

$$\frac{\partial k}{t} + v_i \frac{k}{\partial x_i} = \frac{\partial}{\partial x_i}\left(\frac{\nu_t}{\sigma_k}\frac{\partial k}{\partial x_i}\right) + \nu_t\left(\frac{\partial v_i}{\partial x_j} + \frac{v_j}{\partial x_i}\right)\frac{\partial v_i}{\partial x_j} - \varepsilon$$

$$\frac{\varepsilon}{t} + v_i \frac{\partial \varepsilon}{\partial x_i} = \frac{\partial}{\partial x_i}\left(\frac{\nu_t}{\sigma_\varepsilon}\frac{\varepsilon}{\partial x_i}\right) + C_{1\varepsilon}\frac{\varepsilon}{k}\nu_t\left(\frac{\partial v_i}{\partial x_j} + \frac{v_j}{\partial x_i}\right)\frac{\partial v_i}{\partial x_j} - C_{2\varepsilon}\frac{\varepsilon^2}{k} \quad \text{Equation 4-5}$$

where $\nu_t = C_\mu \frac{k^2}{\varepsilon}$ ≡ local eddy viscosity,

$$\left.\begin{aligned} C_{1\varepsilon} &= 1.44 \\ C_{2\varepsilon} &= 1.92 \\ \text{and } C_\mu &= 0.09 \\ \sigma_k &= 1.0 \\ \sigma_\varepsilon &= 1.3 \end{aligned}\right\} \text{ are universal constants from Launder and Spalding[6].}$$

At a boundary with no-slip, it is not practical to go into the viscous layer, so these are approximated by;

$$k = \frac{v_*^2}{\sqrt{C_\mu}} \quad \text{Equation 4-6}$$

$$\varepsilon = \frac{v_*^3}{\kappa\delta} \quad \text{Equation 4-7}$$

where δ = the effective viscous sub layer thickness,

$$\delta = \frac{12\nu}{v_*} \quad \text{Equation 4-8}$$

In the case of a flow subject to a sudden expansion, as occurs in a vent, there is a very close correlation between the experimental data and the prediction when using the *k*-ε model. The standard *k*-ε model has been subject to many validating experiments, for example Durst and Rastogi[7] amongst others, in a variety of

situations and has proved to be suitable in predicting the flow. Therefore it is highly regarded for general purpose CFD applications.

Advantages and disadvantages of the k-ε model are;

Advantages

- simplest turbulence model for which only initial and or boundary conditions need to be supplied,
- excellent performance for many industrially relevant flows,
- well established; the most widely validated turbulence model.

Disadvantages

- more expensive to implement than mixing length model,
- poor performance in a variety of important cases such as;
    1. some unconfined flows,
    2. flows with large extra strains (eg curved boundary layers),
    3. rotating flows,
    4. fully developed flows in non-circular ducts.

4.4 Salt Water Tank Simulation

With a gravity current in a semi-infinite horizontal box, figure 4-5, the higher density fluid flows in at the bottom, and the lower density fluid flows above this.

This flow is simply due to buoyancy which can be normalised with a positive density difference as;

$$\beta = \frac{(\rho_0 - \rho_1)}{\rho_1} \qquad \text{Equation 4-9}$$

where ρ_0 is the dense ambient fluid, and ρ_1 is the less dense original compartment fluid.

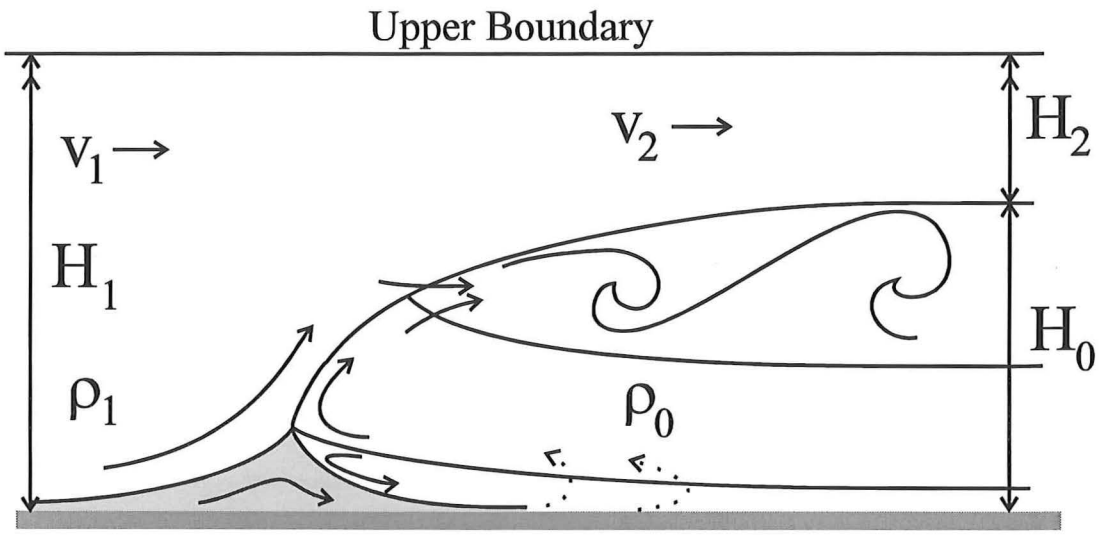

Figure 4-5. Gravity current terms used.

Benjamin[8] uses this, with the assumption of a perfect fluid, with no mixing or diffusion, for the conservation of energy, mass and momentum. This results with;

$$v_1 H_1 = v_2 H_2 \qquad \text{Equation 4-10}$$

$$v_1^2 H_1 + \beta\, g H_1^2 = 2 v_2^2 H_2 + \beta\, g H_2^2 \qquad \text{Equation 4-11}$$

$$v_2^2 = 2\beta\, g(H_1 - H_2 \qquad \text{Equation 4-12}$$

and by solving these equations simultaneously,

$$H_2 = \frac{H_1}{2} = H_0 \qquad \text{Equation 4-13}$$

Then by using equations 4-12 and 4-13, the Froude number for the outgoing fluid is;

$$\frac{v_2}{\sqrt{\beta\, g H_2}} = \sqrt{2} \qquad \text{Equation 4-14}$$

and by then applying equations 4-10, 4-13, and 4-14 with this gives;

$$v^* = \frac{v_1}{\sqrt{\beta\, gH_1}} = \frac{1}{2} \qquad \text{Equation 4-15}$$

the Reynolds number for this flow is simply;

$$Re = \frac{vH_0}{\nu} \qquad \text{Equation 4-16}$$

4.5 References

[1] Fleischmann C. M. *Backdraft Phenomena*, United States Department of Commerce, National Institute of Standards and Technology, NIST-GCR-94-646, June 1994.

[2] Simpson J.E. *Gravity Currents in the Environment and the Laboratory*, Ellis Horwood Limited, 1987.

[3] Schmidt W. *Zur Mechanik der Boen Z.*, Meteorol, Vol 28, 1911, pp 355-362.

[4] Kolmogorov A.N. *Compt Rend Acad Sci* USSR 1941.

[5] Prantl L. *Uber ein neues formeksystem für die ausgebildete turbulenz*, Nach Akad Wiss Göttingen Math-Phys Klasse, 1945, pp 6.

[6] Launder B.E. and Spalding D.B. *The Numerical Computation of Turbulent Flows*, Computer Methods in Applied Mechanics and Engineering, Vol 3, 1974, pp 269-289.

[7] Durst F. and Rastogi A.K. *Theoretical and Experimental Investigations of Turbulent Flows with Separation, in Turbulent Shear Flows*, Springer Verlag, 1979.

[8] Benjamin T.B. *Gravity Currents and Related Phenomenon*, Journal of Fluid Mechanics, Vol 31, 1968, pp 209-248.

5. CFDS-FLOW3D

5.1 Introduction

The FLOW3D[1] software package is a suite of programs used for general modelling of fluid flows, both laminar and turbulent, with or without heat transfer. The current version, release 3.3, is flexible with the "geometry topology" used, utilising a number of coordinate systems.

The overall package is broken down into a number of smaller programs, all of which work together. The package is as follows;

- Pre-processor, *Sophia* where the geometry is drawn using a CAD type interface and the grid is created,
- *Interactive frontend*, where the command language is written, using a point and click approach,
- *CFDS-FLOW3D* or *Astec*, where the data processing is performed,
- Radiation solver *Rad3D*, for use with radiation problems,
- Post-processor, *Flavia* or *Jasper*, which convert the numbers into graphics, or animation, allowing easy representation of the solution.
- *The Environment*, that links all of these programs together and acts like a menu, enabling the user to manoeuvre from one program to another using the mouse.

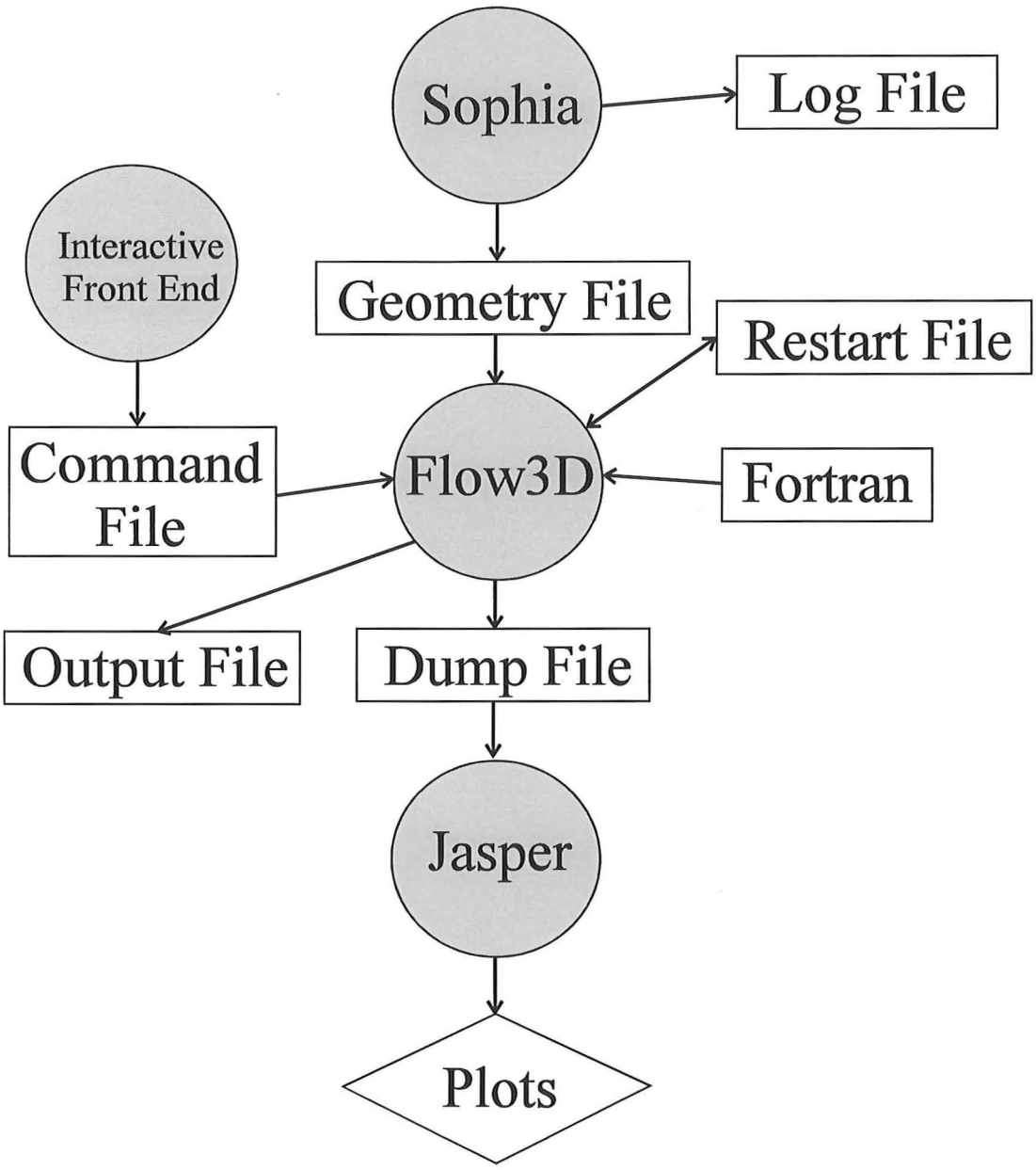

Figure 5-1. The Environment group and relationship of programs.

Flow3D has been in development over a number of years and solves the three dimensional form of the Navier-Stokes equations, for the conservation of mass, momentum and energy, and uses the *k*-ε model, amongst others for turbulence. The physical parameters required by the program in order to do these calculations include density, pressure, specific heat, acceleration due to gravity, thermal conductivity and viscosity. Flow3D is a general purpose CFD program that has been used for modelling smoke flows and other fire simulations. The

current version is capable of determining the products of combustion based on a chemical reaction, and can follow their dispersion in the event of a fire.

The model was used by the developers of the software, Harwell, to investigate the King's Cross underground fire on the 18th of November 1987[2]. In this disaster the fire service and other experts were unable to determine why the fire spread so rapidly. The computer model showed, that in the trench formed with the escalator shaft, the fire would lie down instead of standing upright, contrary to expectations. This phenomenon became known as the "trench effect". Initially this explanation was met with a lot of scepticism from experts, but the phenomenon was later demonstrated conclusively in a number of experiments. The trench effect results from two different phenomena acting in combination. These are the Coanda effect, where the preferential air entrainment for the plume is from below, and the high wind flows induced along the base of the escalator. A traditional zone model, that would normally have been used for the analysis of such a fire, would have provided a significantly different explanation, if one was at all possible.

5.2 Program Familiarisation

Flow3D is presented in a user friendly interface, The Environment version 1.5b, with which it is possible to create the model simply by pointing and clicking the mouse.

The grid generator, Sophia, is a powerful grid generating package. It has the ability to generate the geometry, using a program that is very similar to a typical CAD package. It has the ability to make a number of changes to the topology with relative ease, for instance, a model of two rooms interconnected with a door in which it is possible to change the degree of door opening. These abilities mean that once a geometry is developed, it is relatively easy to make modifications in order to compare the resultant effects.

The Interactive Frontend is well structured for setting appropriate variables, in the command language. In the main, experience has shown that the defaults can be used. A useful feature during entry of variables is the built in checker, it will identify errors that may occur during entry such as specifying a steady state flow but later on specifying transient parameters, or other such incompatible situations. However this checker does not run the command language, so it does not check for errors as for example, having a value set to zero, resulting in a divide by zero error. Although it is possible to create an entire model using the command language, it is generally easier to use Fortran sub-routines and the Sophia grid file. There are a number of User Fortran files already written which are fully commented. This means that modifications, necessary to represent a particular problem are straightforward, even if the user has limited knowledge of Fortran. Familiarity with Fortran is however useful.

The next key area of The Environment is the flow solver. With the package there are two solvers, CFDS-FLOW3D and Astec. The difference between the two is in the nature of grid used. Astec has very little constraint on the grid topology, whereas CFDS-FLOW3D only uses deformed blocks.

The final result from the solver is a dump file that can be read using either Jasper or Flavia, which provide a graphical representation of the solution. The main difference between these two packages is that Flavia has more sophisticated graphical analysis capabilities, and it is possible to create an animation of the flow. Unfortunately this part of the package has not yet been written for the Alpha platform, so it was not possible to use this capability during this study. Jasper provides contour plots with respect to many of the flow parameters, these are more than adequate to obtain a description of the flow field.

5.3 Underlying Theory

The Navier Stokes equations are used for the continuity equation, momentum equation, and energy equation, and have their foundation in Newton's second law of motion. The general form of these equations can be expressed as a scaler advection-diffusion equation, which in coordinate free notation is;

$$\frac{\partial \rho \Phi}{\partial t} + \nabla \cdot \left(\rho v \Phi - \Gamma \nabla \Phi \right) = S \qquad \text{Equation 5-1}$$

where Γ is the diffusion coefficient,

S is the source or sink term representing creation or destruction of Φ.

With turbulence modelling it is impracticable to have a control volume with a size consistent to the phenomena, so turbulence models use estimates known as sub-grid models. The most common turbulence model is the k-ε model, which was originally developed in the seventies and is recognised to be the simplest turbulence model. It is applicable to recirculating flow, which is present in the case of the salt water tank simulations.

The model consists of a buoyancy driven flow and can be modelled in either one of two methods. The first is to use a weakly compressible flow, where the density is calculated using the ideal gas law;

$$\rho = \frac{P}{RT} \qquad \text{Equation 5-2}$$

or, if the temperature difference is small, or there is a small difference in molecular weight, and the compressibility effects are small, then the Boussinesq approximation can be made. These are valid approximations in this case, as it is

assumed that the fluids are at the same temperature and any heating due to viscosity would be minimal.

With the Boussinesq approximation it is assumed that;

$$\rho = \text{constant} = \rho_0 \qquad \text{Equation 5-3}$$

except for in the buoyancy terms for momentum, where thermal expansion is considered, with its effect on density.

With both the compressible flow and the Boussinesq approximation, the calculations of momentum ignore the effect of hydrostatic pressure.

The Boussinesq approximation is simply then;

$$\rho \approx \rho_{ref} \qquad \text{Equation 5-4}$$

provided that ρ_{ref} is chosen so that everywhere in the model $\left|\frac{\partial P}{\partial y}\right| << \rho_{ref} g$, where the P is the pressure without the hydrostatic component.

This arises from the Boussinesq theory as used for modelling horizontal flows. In the model the walls were considered to be adiabatic with no radiative loss away from the tank. This is a reasonable assumption as the water was at ambient temperatures and the only heat source was that due to friction.

The model uses a number of differencing schemes in order to converge to a solution; the most commonly used is the *Upwind* scheme. This is an improvement on the basic scheme as it has the ability to investigate the direction of flow. This is achieved by comparing the value of the property of interest to

the West of the control volume, with respect to the surface of interest. Therefore, if there is a positive difference, the flow will be from West to East, in respect to the cell face. This scheme is conservative, due to the consistent expressions used to calculate the fluxes, but the scheme is only first order accurate as it is based on the backward differencing method. The main limitation with this technique is that it can produce an erroneous result when the flow field does not align with the grid. An improvement on this is the *Hybrid* scheme.

The Hybrid differencing scheme is based on the work of Spalding[3], who combined the Upwind and the basic central differencing schemes. The benefit with this is that the accuracy is improved, to a second order with the central scheme, otherwise it is first order with the application of the Upwind system. These systems are best applied in different flow regimes. The Hybrid scheme therefore has the advantage of being able to exploit the more desirable attributes from the two systems that it is based upon. It is very useful in most common CFD applications.

The SIMPLEC algorithm is based on SIMPLE[4] (Semi-Implicit Method for Pressure-Linked Equations) which is essentially a guess and correct method for calculating the pressure on a staggered grid. This method works by guessing a pressure field and then calculating the resulting velocity components, resulting in a new guess for the pressure. This is repeated until the solution is deemed to have converged. SIMPLEC (SIMPLE + Consistent) is an improvement proposed by Van Doormal and Raithby[5], with modifications to the momentum equations so that the velocity equations ignore the less significant terms.

Once the iterations have converged to a solution on the surface of the cell, it is possible to form a linear differential equation in which to express the value within the cell. This process is known as the inner iteration. In this region it is not necessary for an exact solution as this is only a small step in the overall

iteration process. The simplest method available is the line solver that uses linear relaxation to converge to a solution. This is the default solver for most of the variables used in FLOW3D. Other solvers available include using the preconditioned conjugate gradients, known as the ICCG solver, and Stone's method. Stone[6] considered a variation of the diffusion equation that is strongly implicit. It involves the preliminary matrix factorisation and the solution of a spars-matrix sub-problem, by direct Gaussian elimination[7].

When there is a multi-phase flow, there is one solution field for each phase. The coupled equations that result for the transfer of a characteristic equation between these phases are solved using the SINCE[8] (Simultaneous Solution of Non-linearly Coupled Equations) method.

The boundary conditions for walls specified with no-slip mean that there is zero velocity along these, which eliminates the need to specify the shear stresses involved. In the region near the wall it is necessary to specify a near-wall profile. These can be one of three common variations, linear, quadratic, or logarithmic. The logarithmic profile is generally used for most turbulence regimes, however it is inappropriate for a model with a low Reynolds number turbulence model.

5.4 Creating the Fleischmann Salt Water Tank Model

The process of creating a description of the physical dimensions for the salt water tank simulation, resulted from repeated trial and error. A number of different methods were trialed commencing with detailed specification; initially these were complex and did not represent the problem accurately. With simplification, a working description was created. The result was the basis for developing the Command Language and the User Fortran.

In its simplest form the model can be described as two unequal sized tanks that are connected together. The small tank initially contains fresh water, at 18°C and the larger tank holds salt water at the same temperature, with the ability to change the density of the salt water. The model used is shown in figure 5-2, which gives the general geometry.

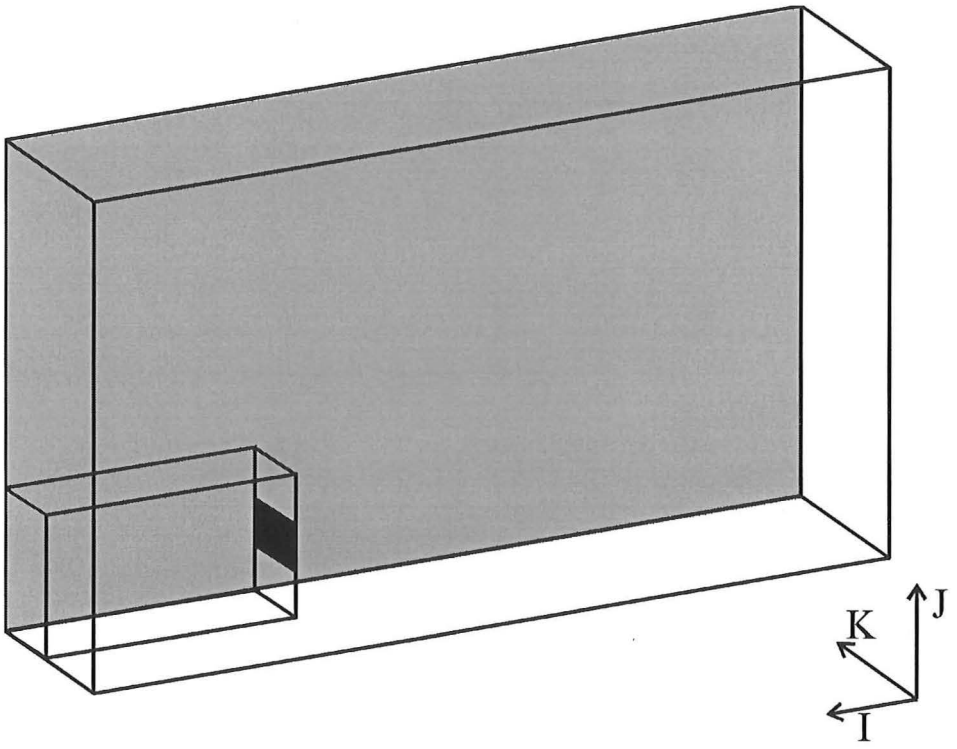

Figure 5-2 Wire frame of the model space, showing the small compartment vent, dark shading, and the plane of symmetry used to reduce computational requirements, light shading.

Figure 5-2 shows the small tank with the vent, inside a larger tank. A plane of symmetry has been used to reduce the necessary time for calculations, which is represented by the light grey shading. The global coordinates I, J, and K are those which were used in the model simulations. The dimensions of the small tank are 300 mm x 150 mm x 75 mm and the large tank 900 mm x 400 mm x 150 mm.

The geometry was improved so as to give a better representation of the actual situation and, with the ability to change the vent size. This was completed by

defining the end plane of the system with a number of faces, and then extruding this along the *x* axis, creating a number of boxes that are linked together.

The vents used in the salt water tank are described in figure 5-3.

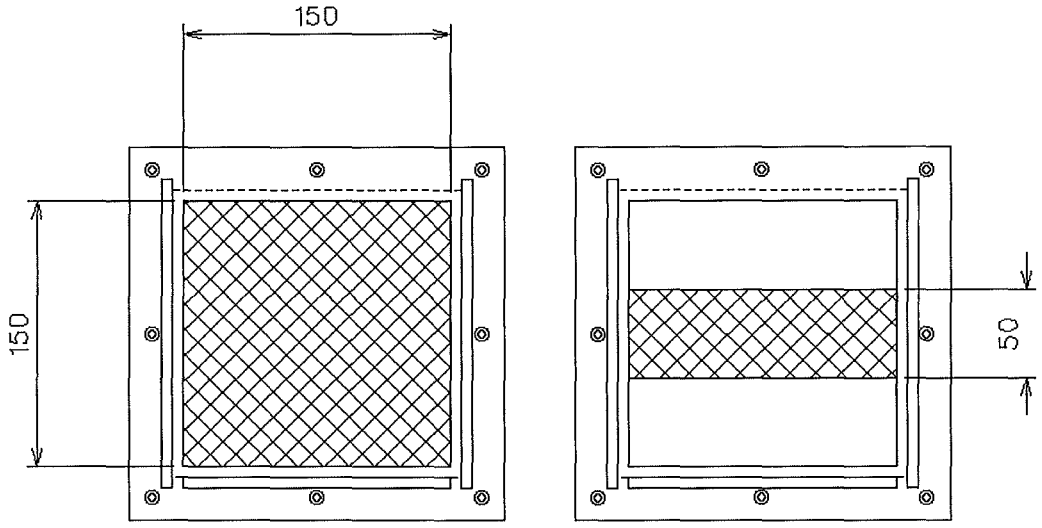

Figure 5-3. Vent geometry used in the salt water tank experiments.

5.5 Method

The process of applying the field model to any situation generally requires a number of different trials at setting the physical description accurately. The working model has been reduced, into seven interconnected blocks, three of which make up the large tank and initially contain salt water and four of which are filled with fresh water and make up the small tank. This arrangement was used to allow flexibility in changing the vent size without having to completely regenerate the grid. The flow was defined as being transient, turbulent, buoyant and incompressible, there by enabling application of the Boussinesq approximation. The initial condition of salt water in one compartment and fresh water in another was set by using a User Fortran file.

The equations were solved using the Upwind differencing scheme. This utilises the upwind cell centre value at each cell face and has the benefit of allowing a quick convergence without introducing significant error.

The buoyancy reference density was set at that of the fresh water, as this is the lighter fluid, and the gravity vector acts along the J plane. Apart from the different densities of the fluids, the fluid parameters were set by using the 'standard fluid' database within the program. The standard k-ϵ turbulence model was used for both fluids.

Figures 5-4, 5-5 and 5-6 show the grid pattern that used in order to get 2,880 control volumes, referred to as 3k. They are identified by the global coordinates IJK, which have been corrected so that I is in the plane of the larger number of cells, for computational efficiency and J is positive upwards, so that the gravity vector is directly in this plane.

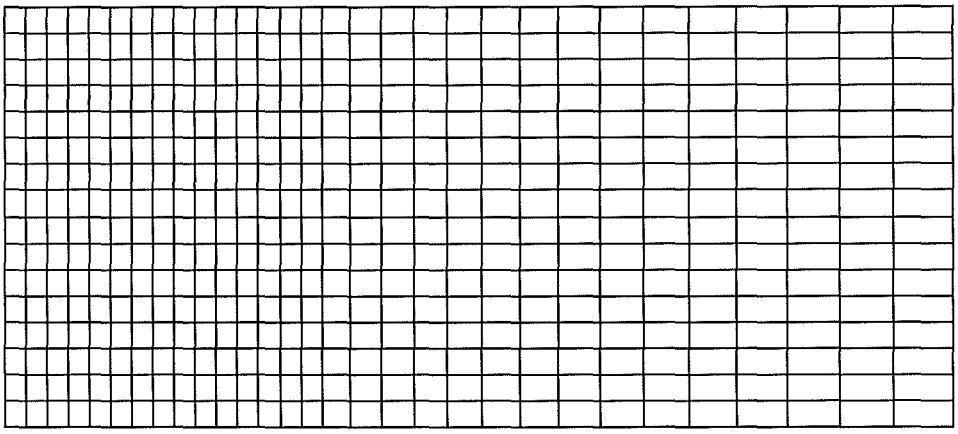

Figure 5-4. IJ view (elevation) showing the initial grid used.

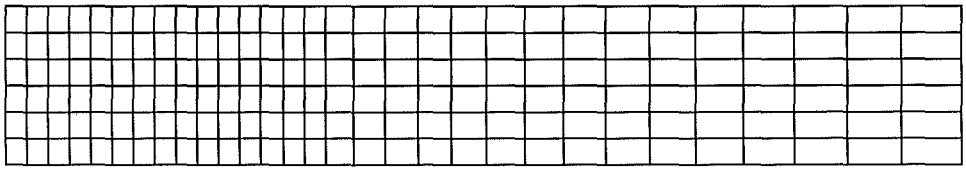

Figure 5-5. IK view (plan) showing the initial grid used.

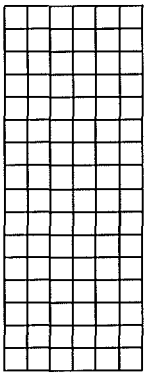

Figure 5-6. JK view (end elevation) showing the initial grid used.

Figures 5-7, 5-8 and 5-9 show the grid pattern that used in order to get 28,800 control volumes, approximated to 30k. This grid pattern was used in the final calculations as it overcame the grid dependence that was present with the previous grid.

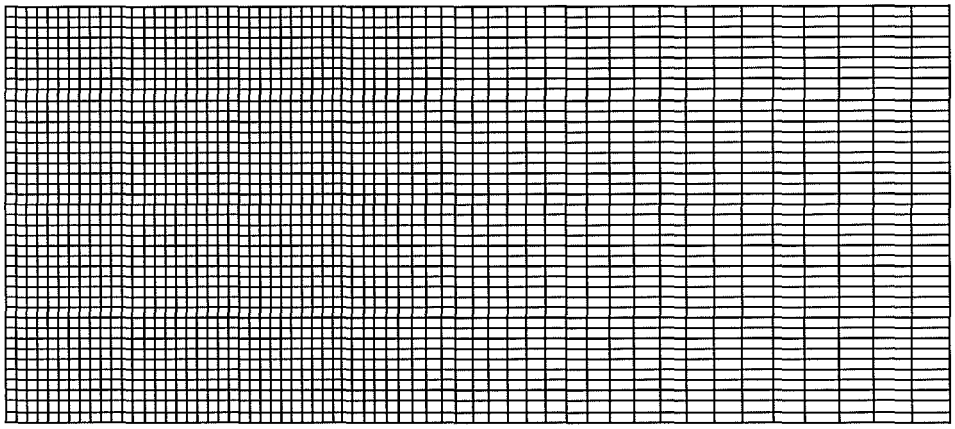

Figure 5-7. IJ view (elevation) showing the final grid used.

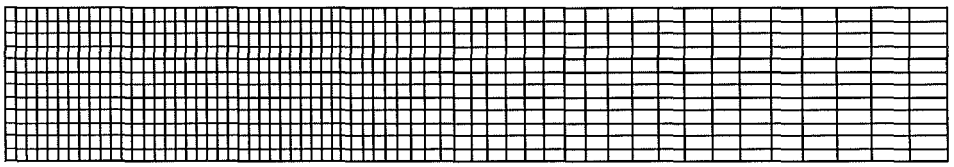

Figure 5-8. IK view (plan) showing the final grid used.

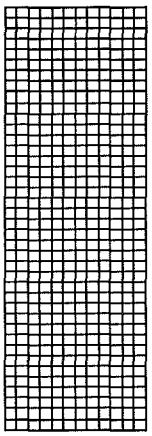

Figure 5-9. JK view (end elevation) showing the final grid used.

5.6 References

[1] Computational Fluid Dynamics Services *FLOW3D Release 3.3: Users Manual*, AEA Technology, Harwell Laboratory, Oxfordshire, United Kingdom, June 1994.

[2] Simcox S., Wilkes N.S. and Jones I.P. *Computer Simulation of the Flows of Hot Gases from the Fire at King's Cross Underground Station*, Fire Safety Journal, Vol 18, 1992, pp 49-73.

[3] Spalding D.B. *A Novel Finite-Difference Formulation for Differential Expressions Involving Both First and Second Derivatives*, International Journal of Numerical Methods Engineering, Vol 4, 1972, pp 551.

[4] Patankar S.V. and Spalding D.B. *Numerical Heat Transfer and Fluid Flow*, Hemisphere Publishing Corporation, Taylor & Francis Group, New York, 1972.

[5] Van Doormal J.P. and Raithby G.D. *Enhancements of the SIMPLE Method for Predicting Incompressible Fluid Flows*, Numerical Heat Transfer, Vol 7, 1984, pp 147-163.

[6] Stone H.L. *Iterative Solution of Implicit Approximations of Multi-Dimensional Partial Differential Equations*, SIAM Journal of Numerical Analysis, Vol 5, No 3, 1968, pp 530-558.

[7] Roache P. J. *Computational Fluid Dynamics*, Hermosa Publishers, Albuquerque, 1972.

[8] Lo S.M. *Mathematical Basis of a Multi-Phase Flow Model*, AERE R 13432, 1989.

6. Step by Step use of the Command Language

6.1 Introduction

The command language is used to define a model and consists of sets of commands and associated key words to define the problem to the solver. There are eight major command sets, and these are discussed below as they were used in this project. This section defines the parameters used in this model and is based on the FLOW3D manual[1].

6.2 Flow3D

This section defines the global parameters used in the model. The first of the sub-commands, `>>SET LIMITS` sets the work space needed by the solver for a particular model.

```
>>FLOW3D
  >>SET LIMITS
    TOTAL INTEGER WORK SPACE 5000000
    TOTAL CHARACTER WORK SPACE 1000
    TOTAL REAL WORK SPACE 18000000
    MAXIMUM NUMBER OF BLOCKS 4
    MAXIMUM NUMBER OF PATCHES 50
    MAXIMUM NUMBER OF INTER BLOCK BOUNDARIES 20
```

The work space is set in this manner so that space is allocated for only what is needed, instead of using all of the space that is available on the computer. The remaining limits control the size of the job.

The next group of sub commands define the type of flow and the environment that the model operates under.

```
>>OPTIONS
  THREE DIMENSIONS
  BODY FITTED GRID
  CARTESIAN COORDINATES
  TURBULENT FLOW
  ISOTHERMAL FLOW
  INCOMPRESSIBLE FLOW
  BUOYANT FLOW
  TRANSIENT FLOW
  NUMBER OF PHASES 2
```

In this case the model is in three dimensions with the grid being body fitted. This is the default grid type and is compatible with all grid forms, whether these are rectangular or orthogonal non-rectangular as would be produced by using Astec.

The nature of the flow is specified, if the flow is turbulent the parameters defining turbulence are accessible within the Frontend, otherwise they are ignored. The flow can be either isothermal or with heat transfer. For this project the fluids were at the same temperature and the boundaries were non-conducting so heat transfer effects could be ignored. The flow can be incompressible, as in the present model, weakly compressible or fully compressible. By using an incompressible fluid the Boussinesq approximation is used.

The flow modelled included buoyancy terms, a time dependence, and two phases. The term phase sets different fluid states, that could be as in classical thermodynamics where the fluid is liquid or a gas, or as different properties of the fluid such as density.

A User Fortran file was used to introduce different algorithms or features that were too complex to set using the command language, for example in this model to define the initial fluid location. Before the User Fortran can be used it is necessary to compile the file before the model is run. The following command preforms this operation, where USRINT is the Fortran procedure called.

```
>>USER FORTRAN
  USRINT
```

6.3 Model Topology

It is possible to represent the geometry using the command language instead of generating a grid file with Sophia. This is a little more complicated, however with simple geometry this method is faster than running Sophia.

If the geometry is drawn in Sophia or Astec, it is necessary to read in this file.

```
>>MODEL TOPOLOGY
  >>INPUT TOPOLOGY
    READ GEOMETRY FILE
```

6.4 Model Data

In this section the physical models and fluid properties were specified.

The accuracy of the model depends, along with numerous other things, on the way in the solution is reached using the differencing scheme. The more accurate schemes tend to be sensitive and slower than the simple schemes. The 'Upwind' differencing scheme is a first order system and investigates the variable to the West of the control volume. This differencing scheme was used as it is a sturdy scheme and has been in use for similar situations with good results.

```
>>MODEL DATA
  >>DIFFERENCING SCHEME
    ALL EQUATIONS 'UPWIND'
    PHASE NAME 'PHASE1'
  >>DIFFERENCING SCHEME
    ALL EQUATIONS 'UPWIND'
    PHASE NAME 'PHASE2'
```

The run title is entered with;

```
  >>TITLE
    PROBLEM TITLE 'TWO BLOCK TANK'
```

The nature of the fluid was specified with the following commands. Water properties are available within the program and those used were at a temperature of 18°C (291 K). The following was the easiest way in which to specify the physical properties of water at this temperature.

```
>>PHYSICAL PROPERTIES
  >>STANDARD FLUID
    PHASE NAME 'PHASE1'
    FLUID 'WATER'
    STANDARD FLUID REFERENCE TEMPERATURE 2.9100E+02
  >>STANDARD FLUID
    PHASE NAME 'PHASE2'
    FLUID 'WATER'
    STANDARD FLUID REFERENCE TEMPERATURE 2.9100E+02
```

With the flow being buoyant it was necessary to specify the direction in which gravity acted. The model had been set up using the vertical direction in the J plane, so the effect of gravity was directly in this plane.

```
>>BUOYANCY PARAMETERS
  PHASE NAME 'PHASE1'
  GRAVITY VECTOR 0.0 -9.8 0.0
  BUOYANCY REFERENCE DENSITY 1.0000E+03
>>BUOYANCY PARAMETERS
  PHASE NAME 'PHASE2'
  GRAVITY VECTOR 0.0 -9.8 0.0
  BUOYANCY REFERENCE DENSITY 1.0000E+03
```

The density of the salt water was changed with the command set that follows. By changing this value the density was changed for the salt water only with all of the remaining properties of water were set with the standard fluid command.

```
>>FLUID PARAMETERS
  PHASE NAME 'PHASE2'
  DENSITY 1.1010E+03
```

The individual phases were required to be defined. In the model the fluid was liquid and continuous in the region of concern, rather than being disperse such as would have been the case of water vapour in the atmosphere.

The multi-phase models were solved with the homogeneous model that assumed that the transported quantities were identical for each fluid except for the volume fraction. This was a satisfactory assumption for conditions with the flow being drag dominated

and where the flow is under gravity. Both these conditions were present in the model. SINCE was used as the default method for accelerating the convergence of the inter-phase coupling equations.

```
>>MULTIPHASE PARAMETERS
  >>PHASE DESCRIPTION
    PHASE NAME 'PHASE1'
    LIQUID
    CONTINUOUS
  >>PHASE DESCRIPTION
    PHASE NAME 'PHASE2'
    LIQUID
    CONTINUOUS
  >>MULTIPHASE MODELS
    >>MOMENTUM
      HOMOGENEOUS
      SINCE
    >>TURBULENCE
      HOMOGENEOUS
      SINCE
    >>CONCENTRATIONS
      INTER PHASE TRANSFER
      SINCE
```

As the flow was time dependant it was modelled at discrete periods of time. The system was studied at ¼ second intervals, up to 10 seconds.

```
>>TRANSIENT PARAMETERS
  >>FIXED TIME STEPPING
    TIME STEPS 40* 2.5E-01
    INITIAL TIME 0.0000E+00
```

6.5 Solver Data

This group of commands controls the solution algorithms.

The model has been set up so that convergence is said to occur if there is 1.0E-6 (0.0001%) difference in the net mass flow terms (kg s^{-1}) during the iteration process. As an additional requirement it was necessary for at least 20 iterations to be performed. In order to limit the computational time a ceiling of 200 iterations was set. In some cases it may be that the iterations do not converge under these operational restrictions in the early time steps however at later times the iterations will tend to be closer and more accurate.

The default equation solvers were used, STONE, ICCG and LINE SOLVER.

```
>>SOLVER DATA
  >>PROGRAM CONTROL
    MAXIMUM NUMBER OF ITERATIONS 200
    MINIMUM NUMBER OF ITERATIONS 20
    OUTPUT MONITOR BLOCK 'SMALL'
    OUTPUT MONITOR POINT 10 1 1
    MASS SOURCE TOLERANCE 1.0000E-06
  >>EQUATION SOLVERS
    ALL PHASES
    U VELOCITY 'STONE'
    V VELOCITY 'STONE'
    W VELOCITY 'STONE'
    PRESSURE 'ICCG'
    VOLUME FRACTION 'STONE'
    K 'LINE SOLVER'
    EPSILON 'LINE SOLVER'
```

6.6 Create Grid

As with the model topology, it is possible to define the grid by using the command language instead of using one of the grid generators. Otherwise the grid file was read in and used.

```
>>CREATE GRID
  >>INPUT GRID
    READ GRID FILE
```

6.7 Model Boundary Conditions

This group of commands defined the real boundary surfaces. In this model there were no boundary conditions of interest and these have not been specified. The vent was modelled as an opening and not as an inlet (or outlet).

```
>>MODEL BOUNDARY CONDITIONS
```

6.8 Output Options

It was necessary to specify what was required in the output file at the end of each run. With this information it was possible to produce line graphs and animations. In the present model only the results for phase 1 (the fresh water) were stored, this was to cut down the size of the dump files produced, as these tended to be very large.

```
>>OUTPUT OPTIONS
  >>DUMP FILE FORMAT
    UNFORMATTED
    SINGLE PRECISION
  >>DUMP FILE OPTIONS
    PHASE NAME 'PHASE1'
    EACH TIME STEP
    FINAL SOLUTION
    ALL VARIABLES
    GEOMETRY DATA
```

6.9 Stop

The final command.

```
>>STOP
```

6.10 Default Parameters

Flow3D uses a number of parameters that are set automatically and therefore have not been included in the above sequence. These are all part of the group of commands under Model Data.

The Backward Difference key word invokes the fully implicit backward Euler differencing scheme for time.

```
>>TRANSIENT PARAMETERS
  >>FIXED TIME STEPPING
    BACKWARD DIFFERENCE
```

Zero velocity conditions along the wall result in the fluid having the same tangential velocity as the wall for all solid boundaries.

```
>>WALL TREATMENTS
  ALL PHASES
  NO SLIP
```

Turbulence is modelled with the standard k-ε model.

```
>>TURBULENCE MODEL
  ALL PHASES
  TURBULENCE MODEL 'K-EPSILON'
```

6.11 User Fortran

The User-Fortran file USRINT, section User5 area is printed below. This defined the areas in which each phase was in at the start of a run.

This section of the file finds the centre of all cell locations and sets the volume fraction (VFRAC) for phase 1 to 1.0. This fills the small block with the fresh water. The remainder of the blocks are similarly filled.

```
C----TO SET UP THE INITIAL FIELD SMALL BLOCKS
C
      FULL=1.0
      EMPTY=1.E-10
C
      CALL IPREC('SMALL','BLOCK','CENTRES',IPT,ILEN,JLEN,KLEN,
     +           CWORK,IWORK)
C
      DO 101 K=1,KLEN
        DO 102 J=1,JLEN
          DO 103 I=1,ILEN
            INODE=IP(I,J,K)
            VFRAC(INODE,1)=FULL
            VFRAC(INODE,2)=EMPTY
 103      CONTINUE
 102    CONTINUE
 101  CONTINUE
```

6.12 References

[1] Computational Fluid Dynamics Services *FLOW3D Release 3.3: Users Manual*, AEA Technology, Harwell Laboratory, Oxfordshire, United Kingdom, June 1994.

7. Results

7.1 Introduction

The computer simulations were preformed using Flow3D Release 3.3 on a DEC Alpha 400 4/233. The control volume computational domain was generally of the order of 30k cells for the final simulations. A typical 10 second simulation with this number of control volumes required up to 19 hours of CPU time.

7.2 Head Shape

The leading edge of the gravity current has a well-defined nose and this is well described in a number of texts. There is no unique shape for the head of a gravity current. This is due to the make up of viscous effects, nature of the ambient flows, and the turbulence in the surroundings. The viscous effects influence the rate of head advancement, and the turbulence will effect the stream along the interface behind the head. One of the best descriptions comes from Simpson[1].

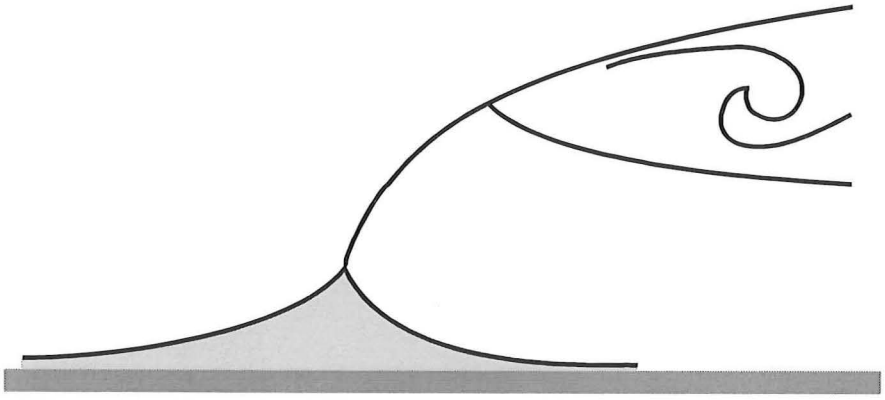

Figure 7-1. Sketch showing the key features of a gravity current, adapted from Simpson.

Figure 7-1 is a sketch of the leading edge of a gravity current showing the characteristic tucking in, where the ambient fluid lifts the nose off the surface. This correlates well with the predicted gravity current from the field model, as shown in figure 7-2.

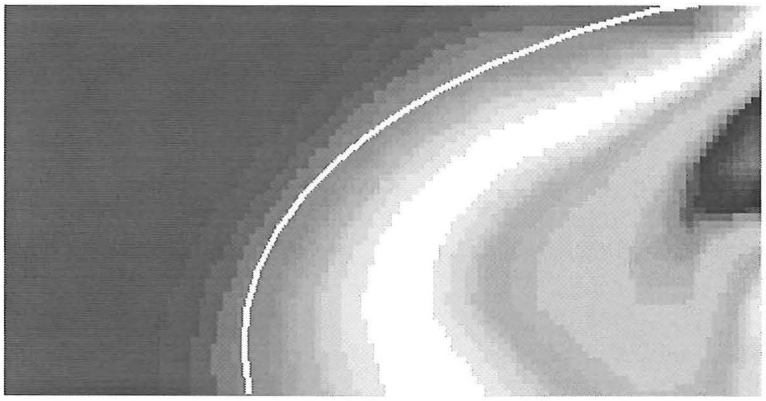

Figure 7-2. CFD graphic of the entering gravity current.

The white line has been superimposed onto the computer image to highlight the nose of the gravity current. This representation suggests that there is a little tucking in at the head of the gravity current.

7.3 Grid Dependence

The effect on the computer solution by the grid size used was perhaps the most significant result found during this investigation. The effect is best described with the following computer images of the predictions with the slot opening and the salt water density of 1101 kg m^{-3}.

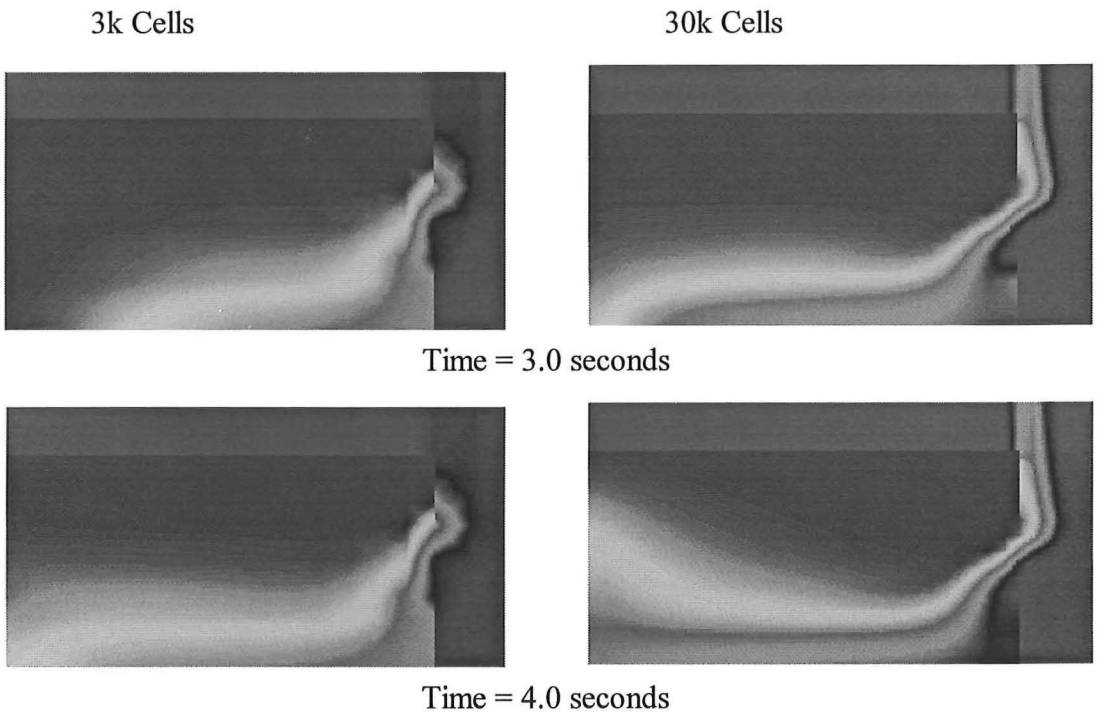

Figure 7-3. Elevation view comparing between different grid sizes.

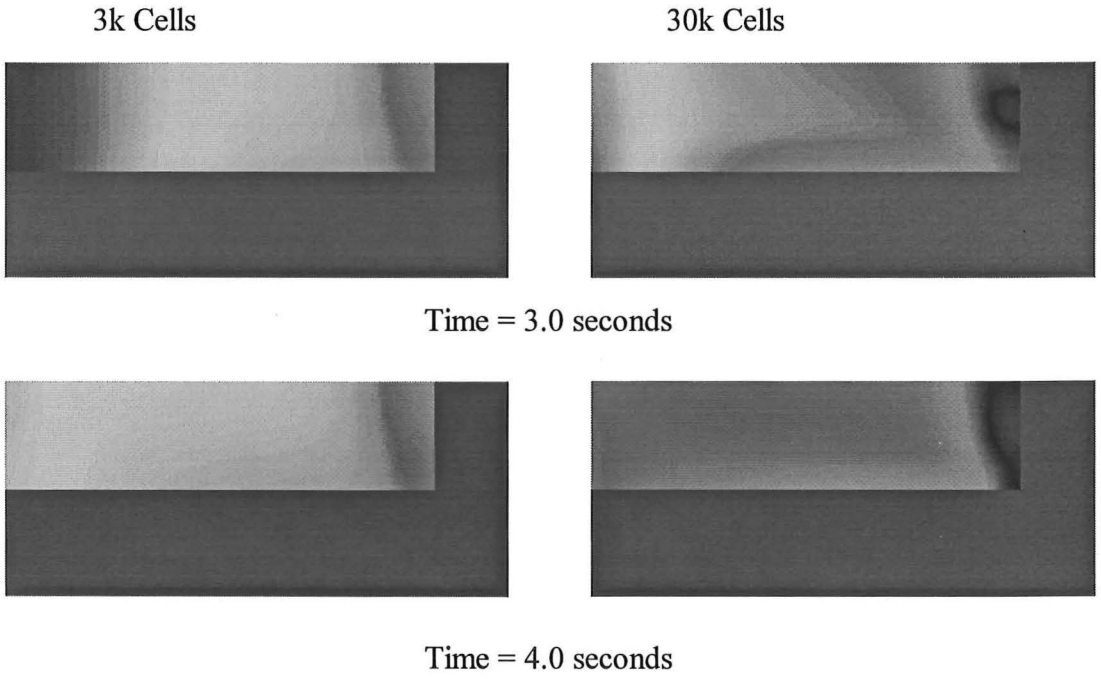

Figure 7-4. Plan view at 20 mm from the bottom surface.

Figure 7-3 is a series of computer images that show the effect of changing the grid size in elevation. Figure 7-4 compares the effect of different girds in a plan view. Figures 7-3 and 7-4 show that after 3 seconds with 30k cells the nose of the gravity current has reached the end wall, while with 3k cells the head has only traveled about 85% of the distance. After an additional second the gravity current has reached the end wall with 3k cells while it has started to develop the return current with the 30k grid.

Figure 7-4 shows the effect of the non-slip boundary condition on the wall surface, that is where the velocity is zero at the wall. This is particularly evident with the 30k grid at 3 seconds. This image shows a region where the flow has been swept back towards the vent, due to this boundary condition.

The main quantitative results when comparing with scaled model salt water tank simulations are the Froude and Reynolds numbers, and height of the entering gravity current.

7.4 Froude Number

The Froude number is used to quantify the relative magnitudes of momentum and buoyancy when they are both are of similar importance. The numerator is proportional to momentum and the denominator proportional to buoyancy.

$$Fr = \frac{v^2}{gD} \qquad \text{Equation 7-1}$$

or as used in salt water tank scaling,

$$v^* = \frac{v}{\sqrt{\beta\, gH}} \qquad \text{Equation 7-2}$$

where,

$$\beta = \frac{(\rho_0 - \rho_1)}{\rho_1}$$ Equation 7-3

This investigation uses the same form of the Froude number as was used in the salt water tank experiments, equation 7-2. The Froude number is dependent on the flow velocity. The velocity was calculated on the basis of the gravity current reaching the end wall in a measurable time. With the distance between the opening and end wall known the velocity can easily be calculated,

$$v = \frac{0.3\ \text{m}}{\text{time (s)}}$$ Equation 7-4

This is at best a crude assumption for the velocity because of the irregularities in direction due to the turbulence present. Therefore a better definition for this is speed, however the gravity current does move in a specific direction, so the velocity is defined on this basis.

The height used in the calculation of the Froude number is that of the compartment, 0.15 m, g is the acceleration due to gravity, and β is defined in equation 7-3.

$$v^* = \frac{0.3}{t\sqrt{\beta \cdot 9.81 \cdot 0.15}}$$ Equation 7-5

where t and β are both known.

Figure 7-5 compares the results with the slot opening of the experimental data (•), with the 30k cells (■), and the 3k cells (◆) simulations, for the Froude number against the relative density. Although both predictions from Flow3D

follow the same trend of the experimental data, there is a significantly better correlation with the 30k grid.

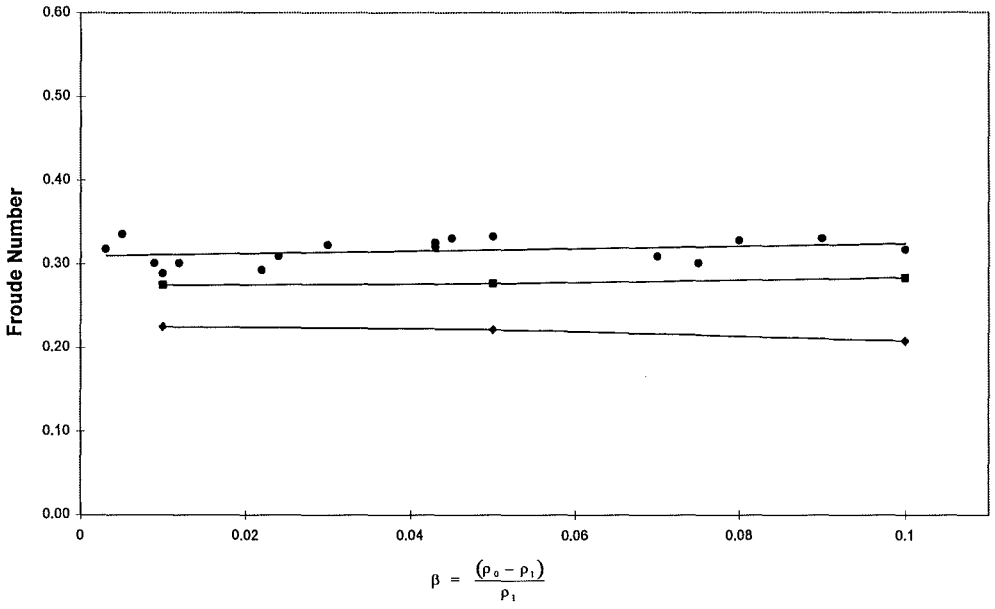

Figure 7-5. Graph with the slot opening comparing the experimental data (•) to the 30k (■) and 3k (♦) predictions for the Froude number.

The experimental data has an error due to the difficulty in measuring the density of the salt water in the laboratory. The required density was calculated by introducing a mass of salt into a known volume of water in the large tank. As a result of these steps, there is an expected error of ±0.06 in the Froude number.

This is highlighted in figure 7-6, where the flow uses the slot opening, and the predicted Froude number from the 30k grid is compared to the experimental data with the error bounds included.

Figure 7-6 shows a very close correlation of the predicted and experimentally obtained Froude numbers, where the prediction lies within the error bounds of the experimentation.

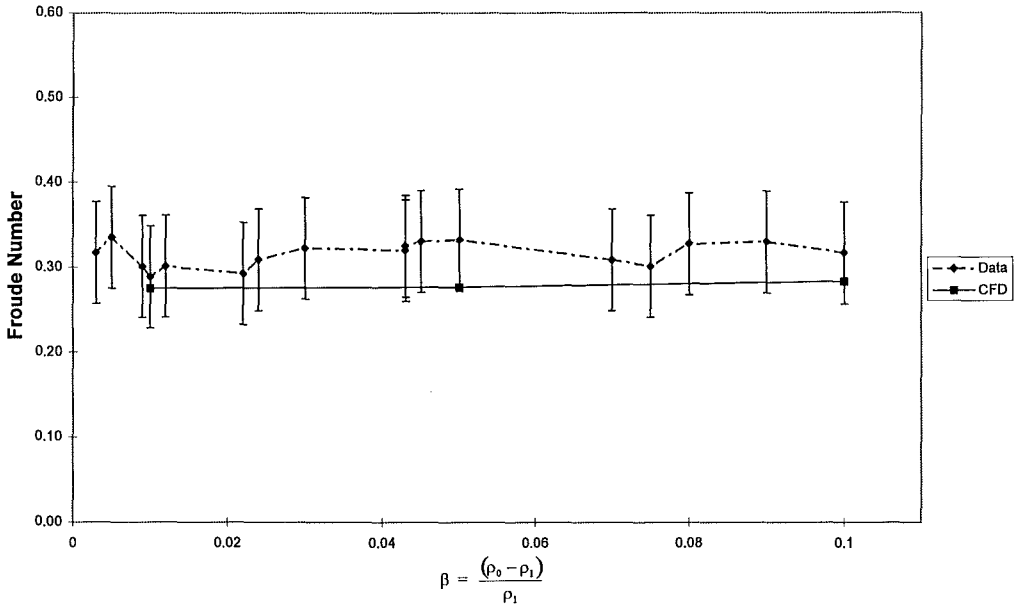

Figure 7-6. Graph of slot opening with the experimental data and the 30k prediction for the Froude number.

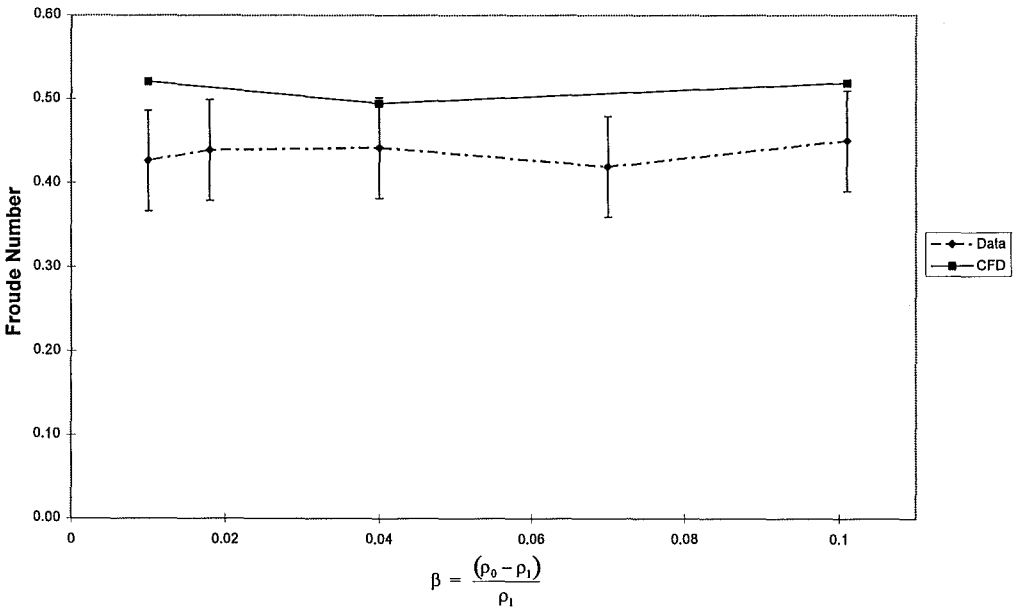

Figure 7-7. Comparison of experimental and predicated Froude numbers with the fully open vent.

With a different vent configuration similarly good results were obtained. Figure 7-7 compares the experimental data to the prediction using the 30k grid with the fully open vent, for the Froude number against the normalised density

difference. This graph does not correlate nearly as well as that with the smaller vent geometry. A likely reason for this would be due to the dependence of the Froude number being calculated by visual observation of time for the gravity current to reach the end wall. The leading edge of the gravity current will be very turbulent, so it will be difficult to accurately know where the nose is. A difference of 0.5 second will result in approximately ±0.05 (15%), depending on the relative density, in the Froude number.

7.5 Reynolds Number

Although the Reynolds number does not have a key role in model scaling, it permits quantitative comparisons of the turbulence within the system. The Reynolds number was calculated by,

$$Re = \frac{vH}{\nu} \qquad \text{Equation 7-6}$$

where v is the velocity, as calculated in equation 7-4
H is the height of the gravity current
ν is the kinematic viscosity

The calculation of the Reynolds number is therefore subject to two visual observations, the time for the gravity current to reach the end wall, and the height of the gravity current. The problems of measuring the time for the velocity have already been mentioned. The height of the gravity current depends on the turbulence down stream of the head. With the slot opening the height could be measured with some accuracy, but with the fully open vent this was not so straight forward as figure 7-8 details.

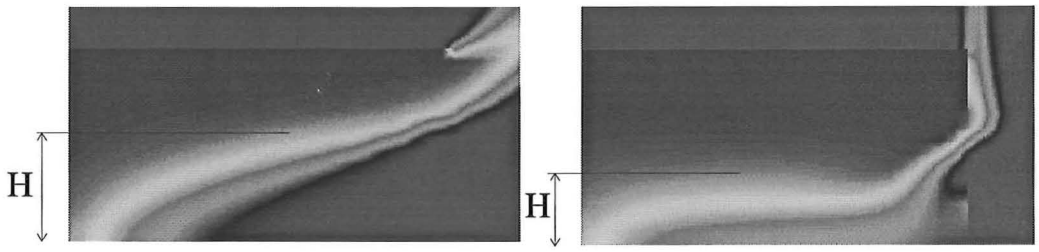

Figure 7-8. Height of the gravity current.

Figure 7-9 compares the results with the slot opening of the experimental data (●), with the 30k cells (■), and 3k cells (◆) simulations, for the Reynolds number against the relative density.

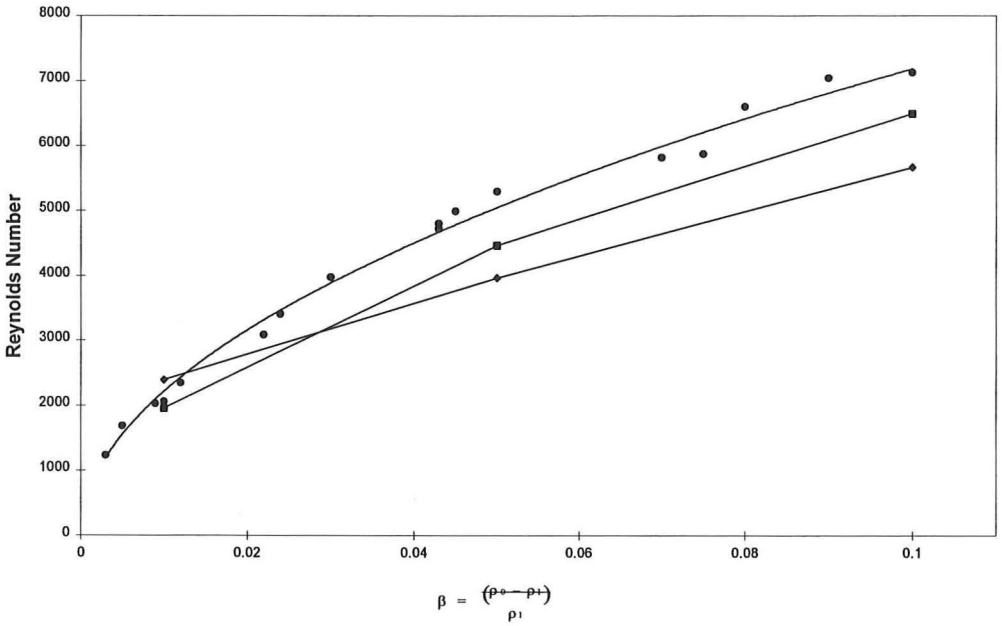

Figure 7-9. Graph with the slot opening comparing the experimental data (●) to the 30k (■) and 3k (◆) predictions for the Reynolds number.

This graph shows again that there is a much better correlation with those results obtained from the 30k grid than those with 3k cells. This is particularly relevant with a low relative density (< 0.05) as below this the 3k grid begins to deviate away from the experimental trend.

Figure 7-10 is the graph obtained with the slot opening of the experimental and predicted results using a 30k grid, for the Reynolds number plotted against the relative density. The results are close, to within 20%, which is very encouraging considering the dependence on observation.

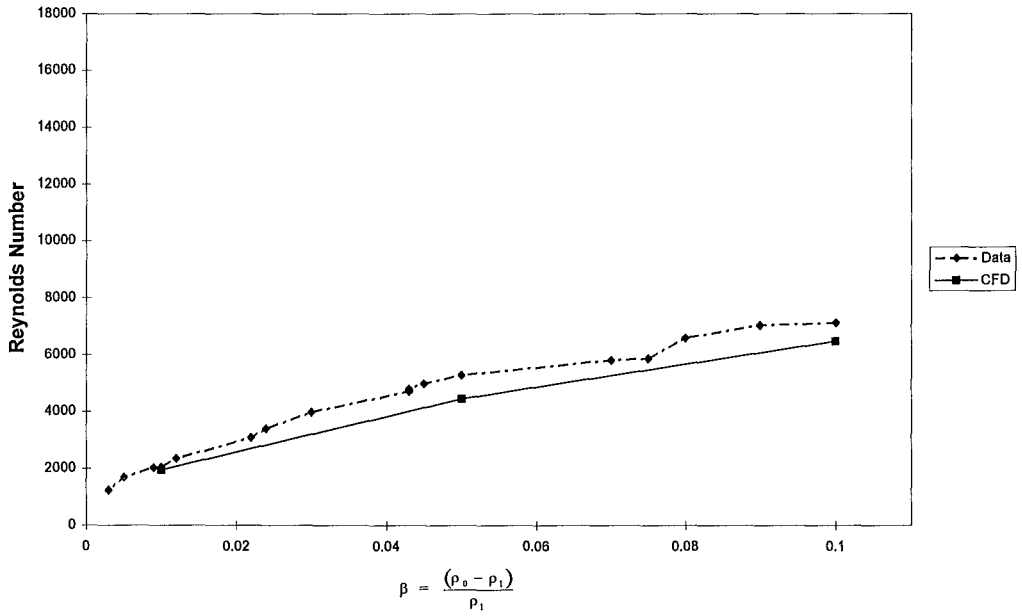

Figure 7-10. Comparison of experimental and predicted Reynolds numbers with the slot opening.

Figure 7-11 shows the effect of changing the vent configuration in the Reynolds number. It consists of the Reynolds number plotted against the relative density for the experiments and the numerical simulations using the 30k cells, with the fully open vent. With a full opening, the flow is much more turbulent, and this is evident both by the difference in Reynolds number as well as with observations.

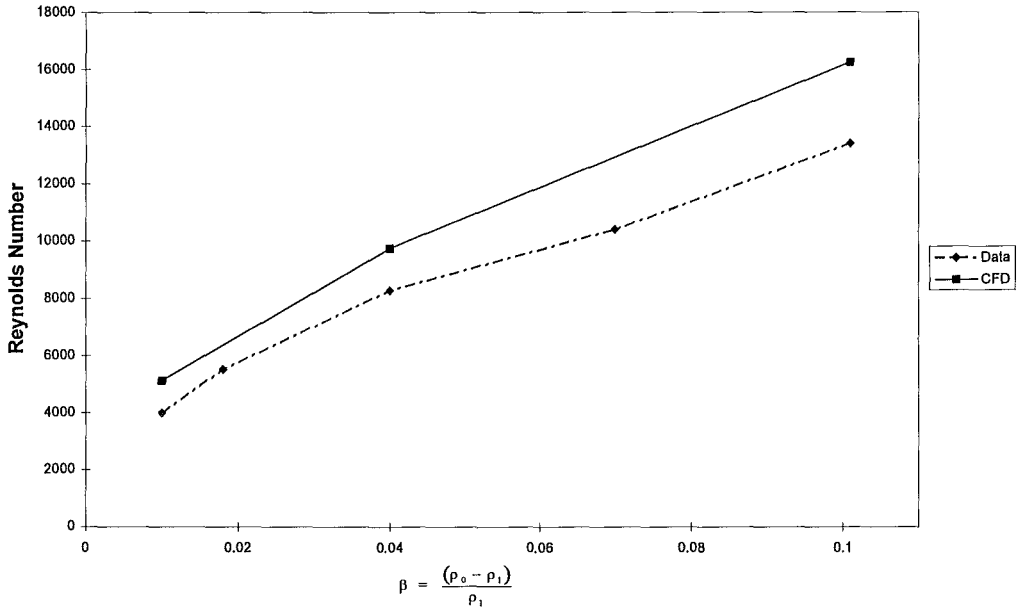

Figure 7-11. Comparison of experimental and predicated Reynolds numbers with the fully open vent.

7.6 Head Height

The height of the entering gravity current when compared to the experimental observations, was used in calculating the Reynolds number.

Table 7-1 summarises the height of the entering gravity current with different vent geometrise.

Vent	Experimental (m)	Predicted (m)
1	0.08	0.09
2	0.06	0.06

Table 7-1. Comparison of entering gravity current head heights with respect to vent opening.

7.7 Iteration Convergence

The following graph, figure 7-12, is a summation of all the residuals modelled, where a residual is the difference between iterations. It shows that in the first nine time steps (2.25 seconds) that the mass residuals do not meet the convergence requirement of 1E-06. They are however all below 1E-05, this arises to a difference in the mass iterations of 0.001%, which is within acceptable limits for this investigation. This graph is characteristic of the simulations with large differences in density, in this example the salt water was at 1101 kg m^{-3} with the horizontal vent. With fluid flows with a lower density salt water, the mass tolerance was reached with fewer iterations, this in-part explains the reduction in computational time for these simulations.

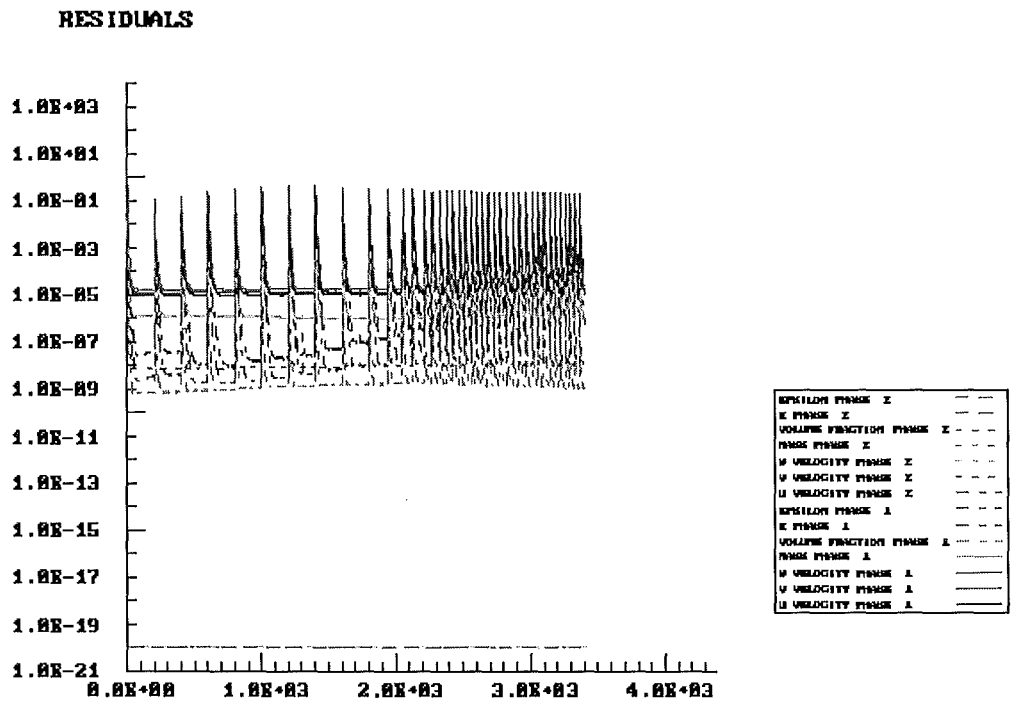

Figure 7-12. Residual plot from horizontal vent opening with $\rho = 1101$ kg m^{-3}.

7.8 References

[1] Simpson J.E. *Gravity Currents in the Environment and the Laboratory*, Ellis Horwood Limited, 1987.

8. Discussion

In general the results from the computer simulations were encouraging as they closely resembled the experimental data that was available.

The Froude number was used to quantify the effects of momentum and buoyancy on a fluid flow. It allows for a direct comparison between results, from the scaled experiments, the salt water tank models and the CFD simulations.

There is a good comparison between the Froude numbers from the salt water tank experiments to the CFD predictions, and these are generally within the error bound of the experimental results. The maximum difference between the experimental and predicted results was 18% (average difference 14%) which is a pleasing result considering the limitations of the experimental data in which the predictions were based.

Although the Reynolds number is not a requirement for the scale accuracy, it has been used in these investigations in order allow a quantitative comparison of the turbulence that is present in the system. The Reynolds number varied from 2,000 with the slot opening and low relative density to over 16,000 for the fully open vent and high relative density. A maximum difference between the predicted and experimental data of 28% was recorded with the full open vent with the density difference of 0.01 kg m^{-3}, and the average deviation was 22%. It is encouraging that there were such good results obtained with the Reynolds number, as this suggests that the flow regime in the CFD simulation was remarkably close to the physical conditions.

The process of measuring the height of the entering gravity current was simple with the slot vent, however with the full open vent the gravity current appeared

to be still developing. So the height used was half the height of the compartment. This is at best a crude assumption, but was used on the basis of the measured height from the experimental data and the expected height predicted from theory.

The effect of grid dependence was noted and can be best described with the comparison of similar models using different grid sizing as found in appendix A. The test for grid dependence was completed as recommended in the Flow3D Users Guide where by the number of cells were doubled in each plane to see if there was any change in solution. This resulted in the number of cells being increased by 2^3, ie from approximately 3,000 to 30,000. Unfortunately due to the limitations on the computer space and time it was not possible to run a simulation with 250,000 cells.

The shape of the leading edge of the gravity current closely matches the general form, where there is tucking in of the leading edge due to there being no-slip along the wall. From the computer image it is not possible to quantify the amount of less dense fluid that flows under the nose of the gravity current.

The rate on which the computer simulation converges to the solution was discussed in an earlier chapter. The solution was said to have converged if there was a difference between iterations of less than 1E-06 in the mass terms. The residual plots of the iteration process show that in the case of the higher difference in fluid densities the process required more iterations in order to meet this criterion. With smaller differences in density the iteration process converged at a much quicker rate, resulting in significantly reduced demands on computer time.

9. Conclusions

The comparison of the Froude number from the Flow3D simulations with the available experimental data compares well with the two different vents modelled. The shape of the entering gravity current with the different opening geometrise, compares well to the observed features from the salt water investigations, and the theory on gravity currents.

With CFD modelling it is necessary to be aware of the effect of grid dependence on the solution. In this project, the initial calculations were completed with 3k cells, which proved to be insufficient in providing an accurate solution. If a larger number of cells had been used at this time, the solution would have been more accurate, but this would have been at the expense of increased computational time. These initial attempts with the command language proved to be better than first thought, because of this dependence.

CFD modelling of smoke flow can provide significant detail of the flow field and has the ability to predict flow patterns within complicated geometrise. The accuracy of the results comes with a significant increase in time, for both setting up the problem as well as tying up the computer resources available. With the ever increasing power of computers, and the development of better software packages, it is foreseeable that in the near future CFD modelling will become more economical for predicting fire and smoke travel in building design.

9.1 Further Work

There were two other vent configurations used in the salt water tank investigations and it would be a relatively simple task to extend the current models so that these other vents could also be modelled.

With the current grid space there is a problem with running out of computer memory that is available. Although it may be possible to work around this problem by changing the computer set-up, it would be interesting to reduce the size of the large tank used in the computer simulations. By so doing, it should be possible to reduce the grid sizing even further, from approximately 12 mm cell faces to 5 mm faces. With this alteration it would be possible to see if the existing model is grid dependent. This increased resolution would enable closer scrutiny of the flow within the vent, as well as the lifting of the gravity current nose. An alternative to making these modifications would be to model the flow in two dimensions instead of three. There have been a number of articles published using only two dimensions for modelling gravity currents and these have provided sufficiently accurate results.

In this project a scaled salt water tank model was used for validation. It would be interesting to compare the results from the computer model to full sized experiments, utilising the combustion algorithm within Flow3D. This could be based on the existing command language with the necessary modifications for the changes in geometry, and use of the combustion model. It is suggested that the gravity current be modelled using a natural gas burner as the heat source, so that the chemical equations are simple, and the effects of the products of combustion on radiation will be minimal.

10. References

Babrauskas V. *A Closed-form Approximation for Post-Flashover Compartment Fire Temperatures*, Fire Safety Journal, Vol 4, 1981, pp 63-73.

Backdraft: A Horrible Reality that Kills or Maims in Seconds, Fire Fighting in Canada, April-May, 1980, pp 4-5.

Baum H.R., Cassel K.W., McGrattan K.B. and Rehm R.G. *Gravity-Current Transport in Building Fires*, Proceedings International Conference on Fire Research and Engineering, 1995, pp 27-32.

Benjamin T.B. *Gravity Currents and Related Phenomenon*, Journal of Fluid Mechanics, Vol 31, 1968, pp 209-248.

Bilger R.W. *Computational Field Models in Fire Research and Engineering*, Fire Safety Science Proceedings of the Fourth International Symposium, 1994, pp 95-110.

Blottner F.G. *Non-equilibrium Laminar Boundary-Layer Flow of Ionised Air*, AIAA Journal, Vol 2, No. 11, November 1964, pp 1921-1927.

Bolliger I. *Full Residential Scale Backdraft*, Masters Thesis, Department of Civil Engineering, University of Canterbury, Christchurch, New Zealand, 1995.

Buchannan A. (Editor) *Fire Engineering Design Guide*, Centre of Advanced Engineering, University of Canterbury, July 1994.

Bukowski R.W. *Modelling a Backdraft: The Fire at 62 Watts Street*, NFPA Journal, Nov/Dec 1995, pp 85-89.

Computational Fluid Dynamics Services *FLOW3D Release 3.3: Users Manual*, AEA Technology, Harwell Laboratory, Oxfordshire, United Kingdom, June 1994.

Courant R. Friedrichs K.O. and Lewy H. *Uber die Partiellen Differenzengleichurgen der Mathematischen Physik*, Mathematische Annalen, Vol 100, 1928, pp 32-74

Davis W.D. Forney G.P. and Bukowski R.W. *Field Modeling: Simulating the Effect of Sloped Beamed Ceilings on Detector and Sprinkler Response*, International Fire Detection Research Project, National Fire Protection Research Foundation, 1994.

Davis W.D. Forney G.P. and Klote J.H. *Field Modeling of Room Fires*, United States Department of Commerce, National Institute of Standards and Technology, NISTIR 4673, 1991.

Durst F. and Rastogi A.K. *Theoretical and Experimental Investigations of Turbulent Flows with Separation, in Turbulent Shear Flows*, Springer Verlag, 1979.

Fatal Mattress Store Fire At Chatham Dockyard, Fire, 67, 388, 1975.

Fay J.A. and Riddell F. R. *Theory of Stagnation Point Heat Transfer in Dissociated Air*, Journal of the Aeronautical Sciences, Vol 25, No 2, February 1958, pp 73-85.

Fleischmann C. M. *Backdraft Phenomena*, United States Department of Commerce, National Institute of Standards and Technology, NIST-GCR-94-646, June 1994.

Forney G.P. Bukowski R.W. and Davis W.D. *Field Modeling: Effects of Flat Beamed Ceilings on Detector and Sprinkler Response*, National Fire Protection Research Foundation, 1993.

Hadjisophocleous G.V. and Cacambouras M. *Computer Modeling of Compartment Fires*, Journal of Fire Protection Engineering, Vol 5, No 2, 1993, pp 39-52.

Jassens M. *Room Fire Models Heat Release in Fires* (Babrauskas V. and Grayson S.J. Editors), Elseiver Science Publishers Ltd, London, 1992, pp 113-157.

Kerrison L. Galea E.R. Hoffman N. and Patel M.K. *A Comparison of a FLOW3D Based Fire Field Model with Experimental Room Fire Data*, Fire Safety Journal, Vol 23, No 4, 1994, pp 387-411.

Kolmogorov A.N. *Compt Rend Acad Sci* USSR 1941.

Kopal Z. *Tables of Supersonic Flow Around Cones*, Department of Electrical Engineering, Centre of Analysis, Massachusetts Institute of Technology, Cambridge, 1947.

Kumar S. *Field Model Simulations of Vehicle Fires in a Channel Tunnel Shuttle Wagon*, Fire Safety Science Proceedings of the Fourth International Symposium, 1994, pp 995-1006.

Launder B.E. and Spalding D.B. *The Numerical Computation of Turbulent Flows*, Computer Methods in Applied Mechanics and Engineering, Vol 3, 1974, pp 269-289.

Leendertse J.J. (Discussion in,) *Transient Models for Inland Coastal Waters* (by H.B. Fisher), Academic Press, 1981.

Lo S.M. *Mathematical Basis of a Multi-Phase Flow Model*, AERE R 13432, 1989.

Lockwood F.C. and Malalasekera W.M.G. *Fire Computation: The 'Flashover' Phenomenon*, Twenty-Second Symposium (International) on Combustion, The Combustion Institute, 1988, pp 1319-1328.

Markatos N.C. Malin M.R. and Cox G. *Mathematical Modeling of Buoyancy Induced Smoke Flow in Enclosures*, International Journal of Heat and Mass Transfer, Vol 25, No 1, 1982, pp 63-75.

Mawhinney R.N. Galea E.R. Hoffmann N. and Patel M.K. *A Critical Comparison of a Phoenics Based Fire Field Model with Experimental Compartment Data*, Journal of Fire Protection Engineering, Vol 6, No 4, 1994, pp 137-152.

McCaffrey B.J. Quintiere J.G. and Harkleroad M.F. *Estimating Room Fire Temperatures and the Likelihood of Flashover Using Fire Test Data Correlations*, Fire Technology, Vol 12, No 2, 1981, pp 98-119.

Millar D. *Full Scale Limited Ventilation Fire Experiments*, University of Canterbury Masters of Fire Engineering Thesis, 1995.

Moretti G. and Abbett M. *A Time Dependent Computational Method for Blunt Body Flows*, AIAA Journal, Vol 4, No 12, December 1966, pp 2136-2141.

Nam S. and Bill R.G. *Numerical Simulation of Thermal Plumes*, Fire Safety Journal, Vol 21, 1993, pp 231-256.

Notarianni K.A. and Davis W.D. *The Use of Computer Models to Predict Temperature and Smoke Movement in High Spaces*, United States Department of Commerce, National Institute of Standards and Technology, NISTIR 5304, 1993.

Patankar S.V. and Spalding D.B. *Numerical Heat Transfer and Fluid Flow*, Hemisphere Publishing Corporation, Taylor & Francis Group, New York, 1972.

Prantl L. *Uber ein neues formeksystem für die ausgebildete turbulenz*, Nach Akad Wiss Göttingen Math-Phys Klasse, 1945, pp 6.

Phillips H. and Wiener N. *Nets and the Dirichlet Program*, Journal of Mathematics and Physics, Vol 2, 1923, pp 105-124.

Richardson L.F. *The Approximate Arithmetical Solution of Finite Differences of Physical Problems Involving Differential Equations, with an Application to the Stresses in a Masonry Dam*, Transactions of the Royal Society of London, Ser A, Vol 210, 1910, pp 307-357.

Roache P. J. *Computational Fluid Dynamics*, Hermosa Publishers, Albuquerque, 1972.

Russel D. Seven Fire Fighters Caught in Explosion, Fire Engineering, April 1983, pp 22-23.

Schaelin A., van der Maas J. and Moser A. *Simulation of Airflow Through Large Openings in Buildings*, ASHRAE Transactions: Symposia, Vol 98, part 2, 1992, pp 319-328.

Schmidt W. *Zur Mechanik der Boen Z.*, Meteorol, Vol 28, 1911, pp 355-362.

Simcox S., Wilkes N.S. and Jones I.P. *Computer Simulation of the Flows of Hot Gases from the Fire at King's Cross Underground Station*, Fire Safety Journal, Vol 18, 1992, pp 49-73.

Simpson J.E. *Gravity Currents in the Environment and the Laboratory*, Ellis Horwood Limited, 1987.

Simpson J.E. *Gravity Currents in the Laboratory, Atmosphere, and Ocean*, Annual Review of Fluid Mechanics, Vol 14, 1982, pp 213-234.

Spalding D.B. *A Novel Finite-Difference Formulation for Differential Expressions Involving Both First and Second Derivatives*, International Journal of Numerical Methods Engineering, Vol 4, 1972, pp 551.

Southwell R.V. *Relaxation Methods in Theoretical Physics*, Oxford University Press, New York, New York, 1946.

Stone H.L. *Iterative Solution of Implicit Approximations of Multi-Dimensional Partial Differential Equations*, SIAM Journal of Numerical Analysis, Vol 5, No 3, 1968, pp 530-558.

Stroup D.W. *Using Field Modeling to Simulate Enclosure Fires*, SFPE Handbook, 2nd Edition, Section 3, Chapter 8, 1995, pp 152-159.

Thom A. *The Flow Past Circular Cylinders at Low Speeds*, Proceedings of the Royal Society of London, A141, 1933, pp 651-666.

Thomas P.H. *Testing Products and Materials for their Contribution to Flashover in Rooms*, Fire and Materials, Vol 5, No 3, 1981, pp 103-111.

Tubbs J.S. and Barnett J. *Modeling the NIST High Bay Fire Experiment with Jasmine*, Proceedings of the International Conference on Fire Research and Engineering, 1995, pp 383-388.

Van Doormal J.P. and Raithby G.D. *Enhancements of the SIMPLE Method for Predicting Incompressible Fluid Flows*, Numerical Heat Transfer, Vol 7, 1984, pp 147-163.

Walton W.D. and Thomas P.H. *Estimating Temperatures in Compartment Fires*, SFPE Handbook, Section 2, Chapter 2, 1992, pp 16-32.

Waterman T.E. *Room Flashover- Criteria and Synthesis*, Fire Technology, Vol 4, 1968, pp 113-157.

Appendix A

The following images show the volume fractions as a function of time with two different grid sizes. The slot opening was used with a salt water density of 1101 kg m^{-3} and the images were taken in the IJ plane (elevation) near the plane of symmetry.

3,000 Cells $\rho = 1101$ kg m^{-3} 30,000 Cells $\rho = 1101$ kg m^{-3}

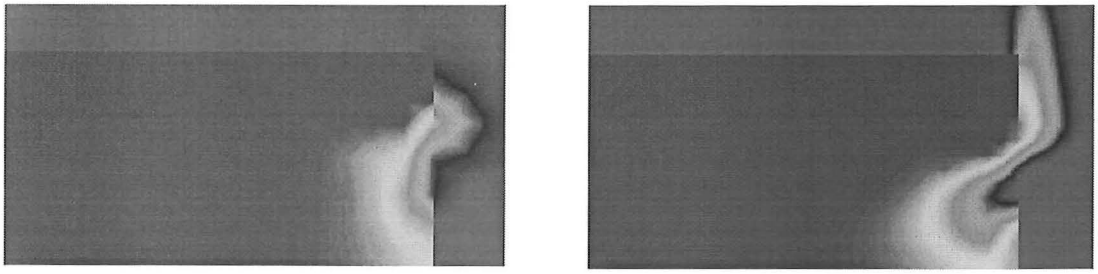

Time = 1.0 seconds

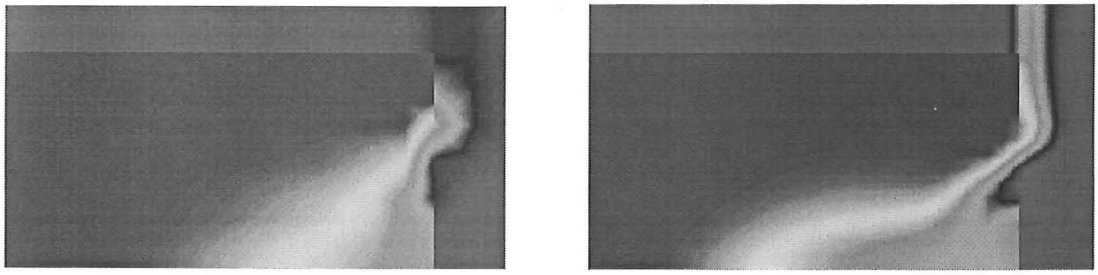

Time = 2.0 seconds

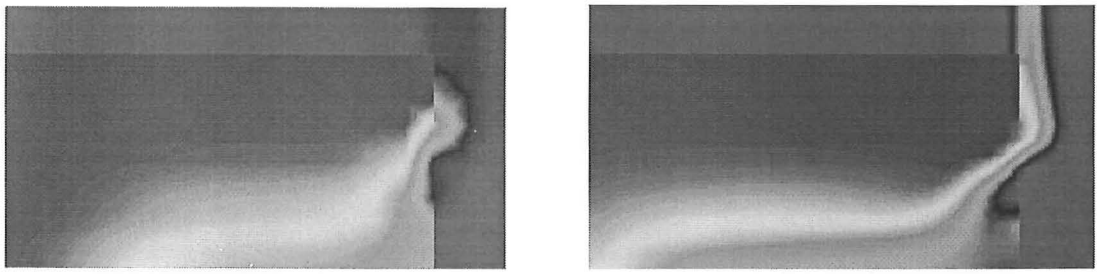

Time = 3.0 seconds

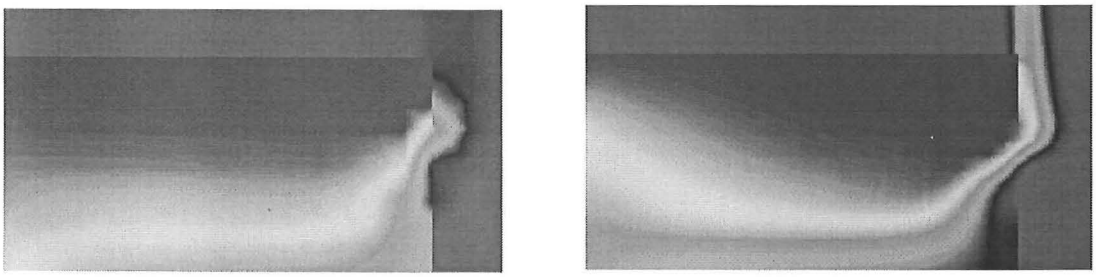

Time = 4.0 seconds

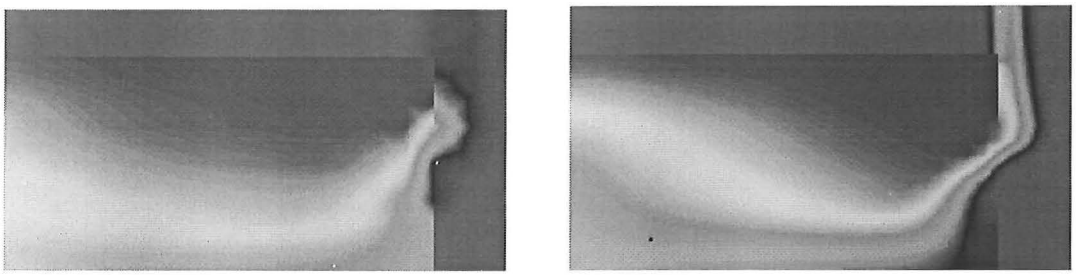

Time = 5.0 seconds

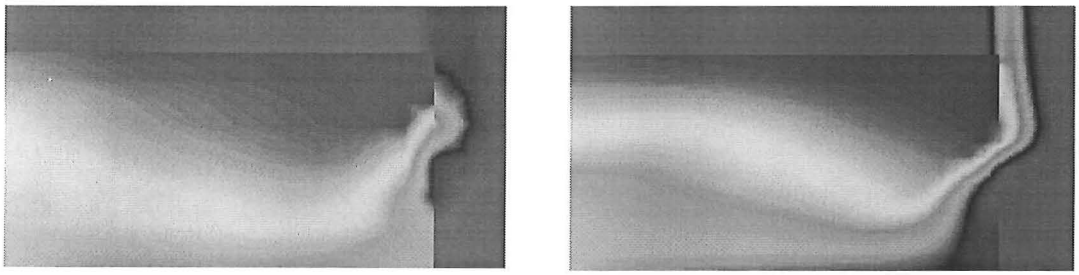

Time = 6.0 seconds

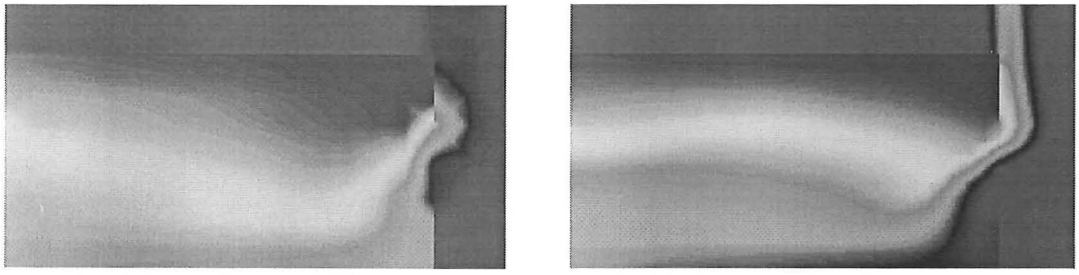

Time = 7.0 seconds

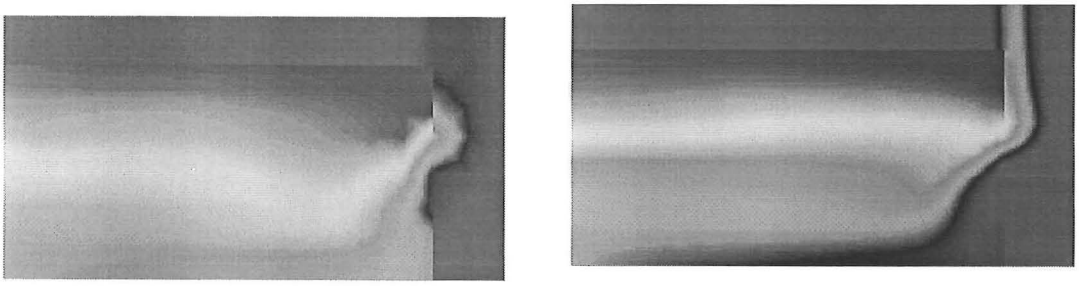

Time = 8.0 seconds

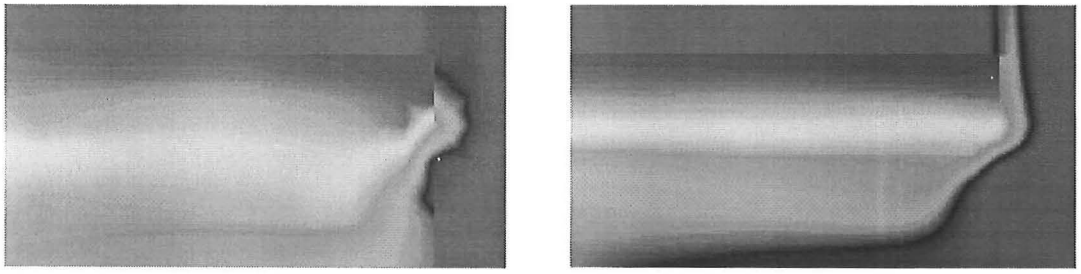

Time = 9.0 seconds

The following images are taken in the IK (plan) view, 20 mm from the base of the small tank.

3,000 Cells $\rho = 1101$ kg m^{-3}

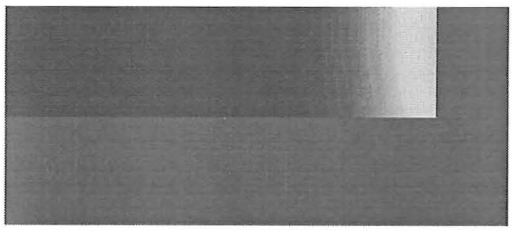

30,000 Cells $\rho = 1101$ kg m^{-3}

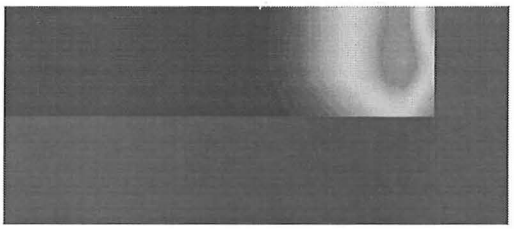

Time = 1.0 seconds

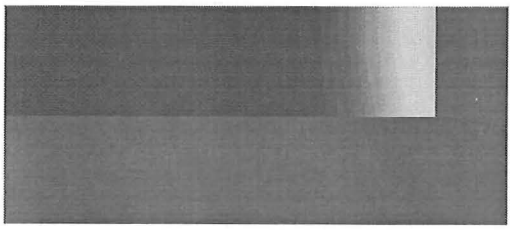

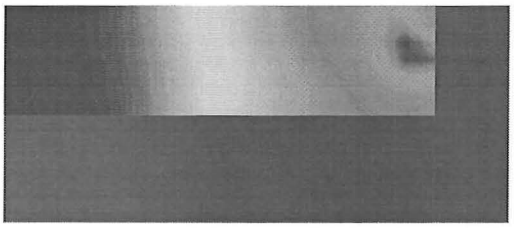

Time = 2.0 seconds

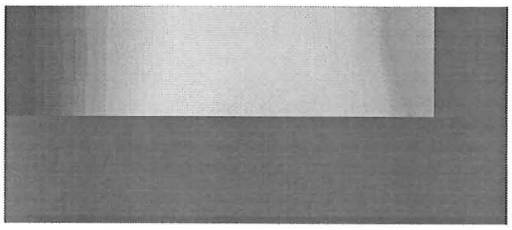

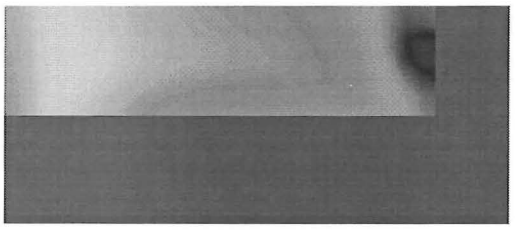

Time = 3.0 seconds

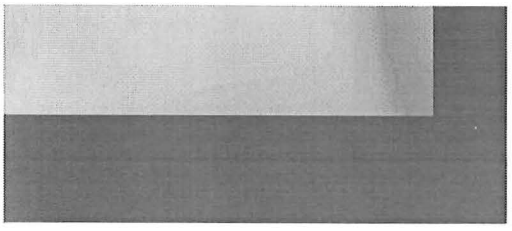

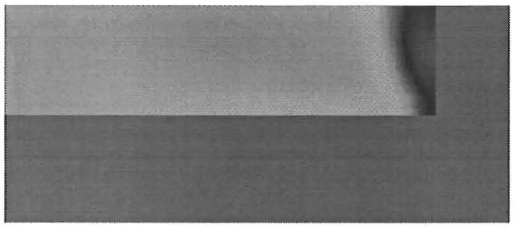

Time = 4.0 seconds

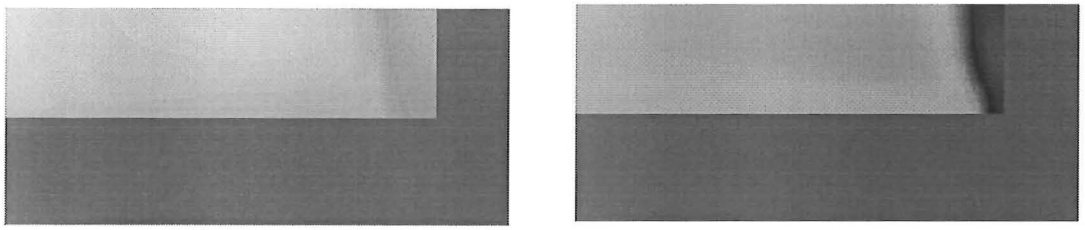

Time = 5.0 seconds

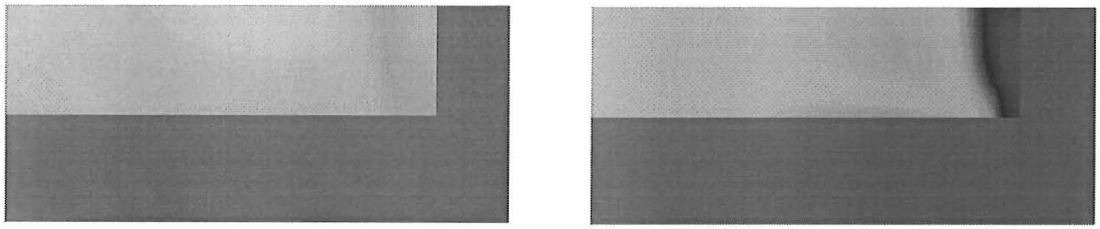

Time = 6.0 seconds

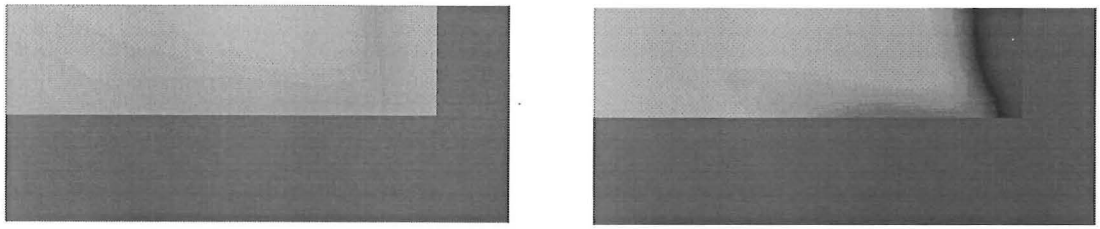

Time = 7.0 seconds

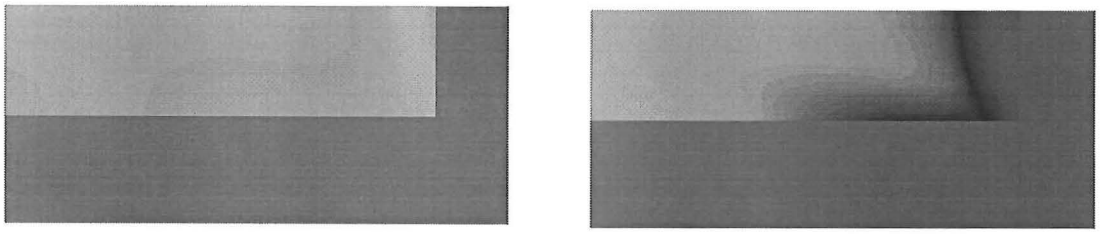

Time = 8.0 seconds

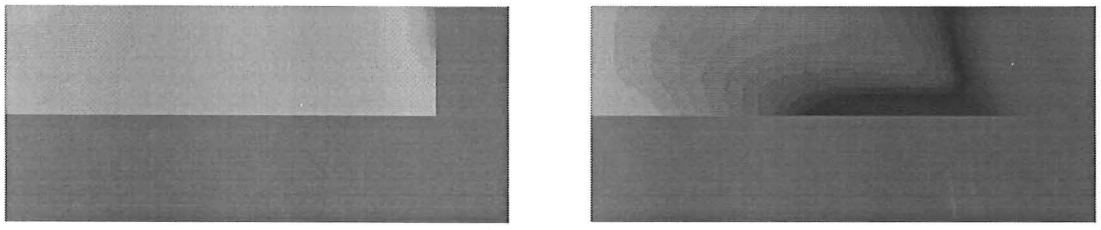

Time = 9.0 seconds

Appendix B

The output from the fully open vent are presented below in second intervals. The first group use a salt water density of 1101 kg m^{-3}.

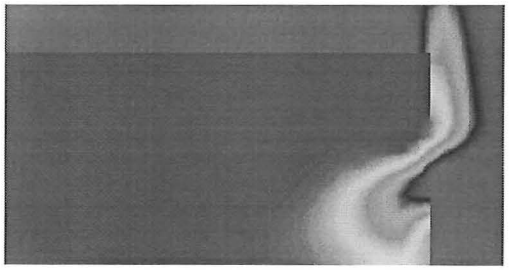

Time = 1.0 second

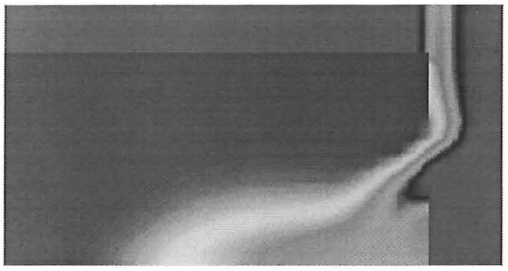

Time = 2.0 seconds

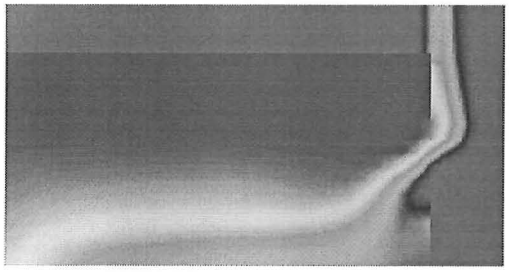

Time = 3.0 seconds

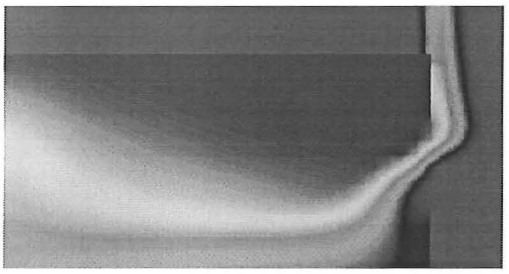

Time = 4.0 seconds

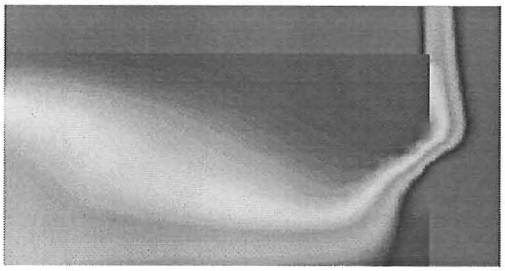

Time = 5.0 seconds

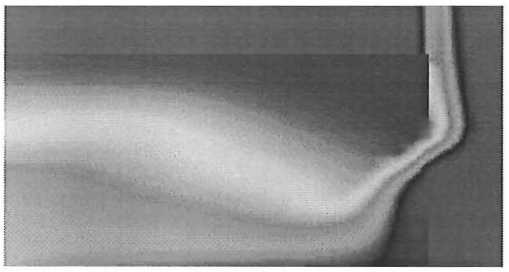

Time = 6.0 seconds

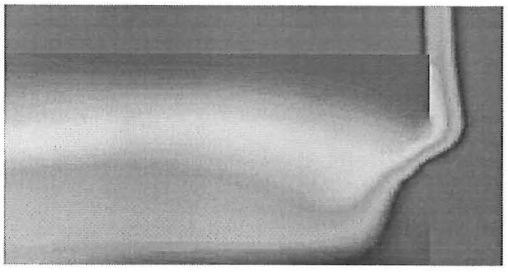

Time = 7.0 seconds

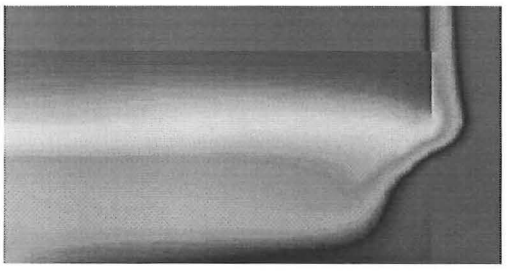

Time = 8.0 seconds

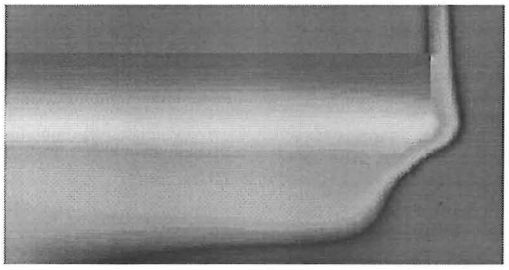

Time = 9.0 seconds

The following images are taken with the salt water density of 1050kg m^{-3}.

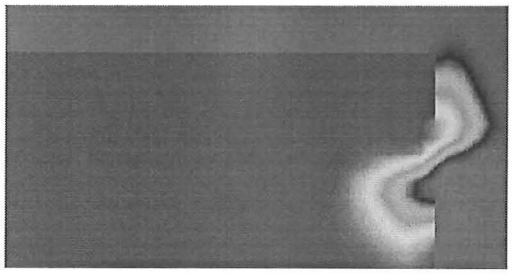

Time = 1.0 second

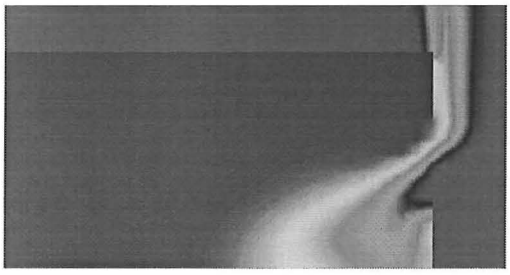

Time = 2.0 seconds

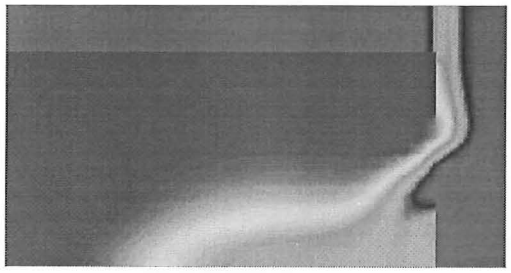

Time = 3.0 seconds

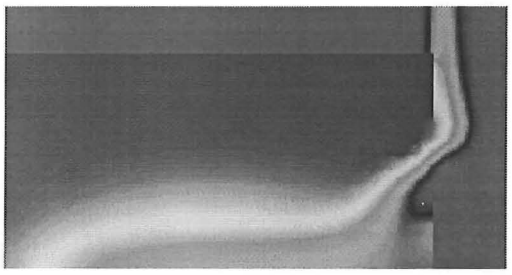

Time 4.0 seconds

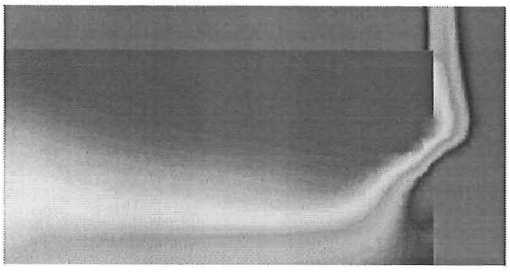

Time = 5.0 seconds

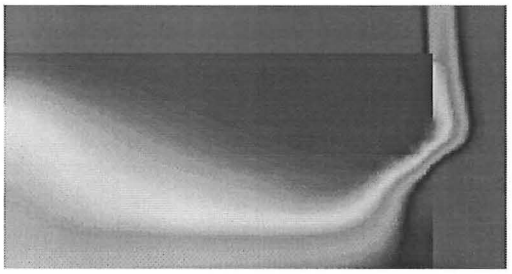

Time = 6.0 seconds

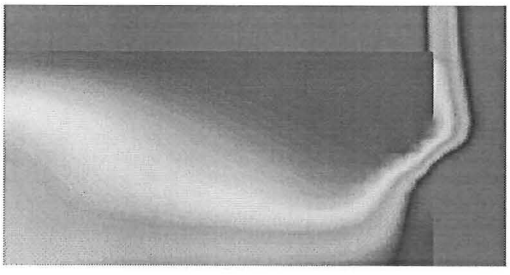

Time = 7.0 seconds

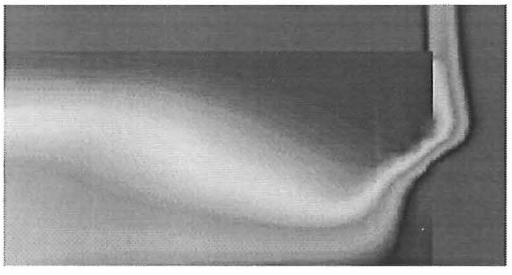

Time = 8.0 seconds

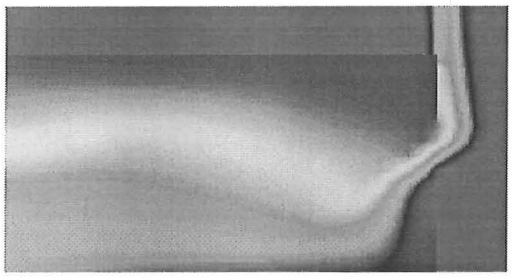

Time = 9.0 seconds

The following images are taken with the salt water density of 1010 kg m^{-3}.

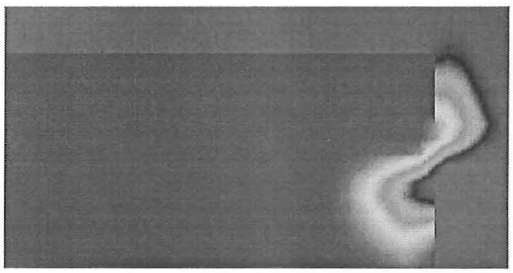

Time = 1.0 second

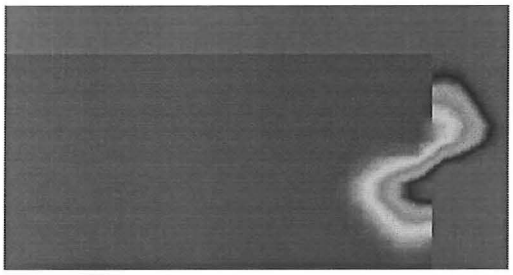

Time = 2.0 seconds

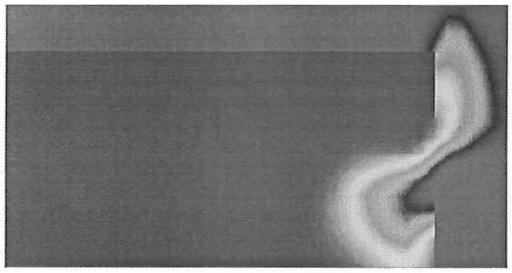

Time = 3.0 seconds

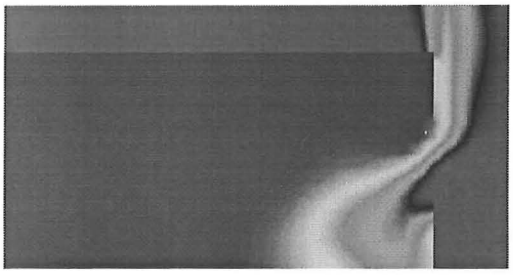

Time = 4.0 seconds

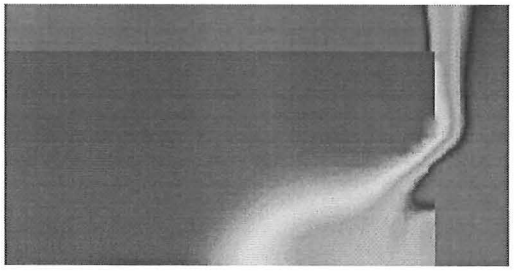

Time = 5.0 seconds

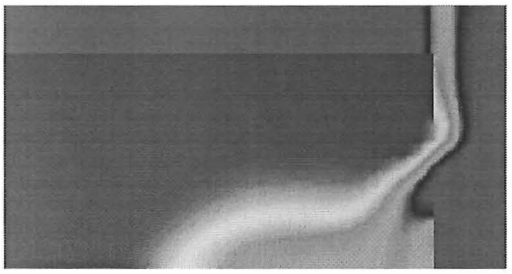

Time 6.0 seconds

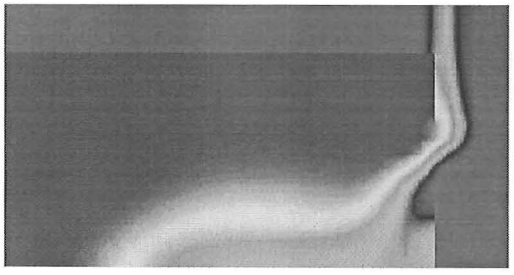

Time = 7.0 seconds

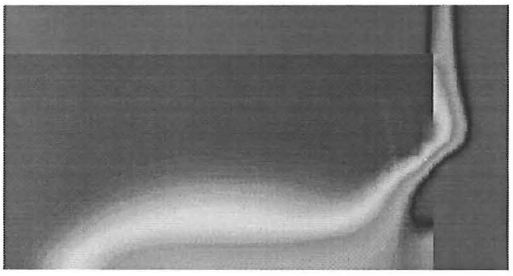

Time 8.0 seconds

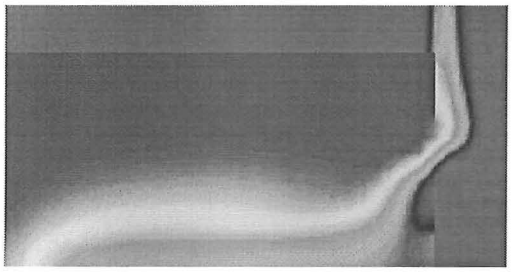

Time = 9.0 seconds

Appendix C

The output from the slot opening vent are presented below in second intervals. The first group use a salt water density of 1101 kg m^{-3}.

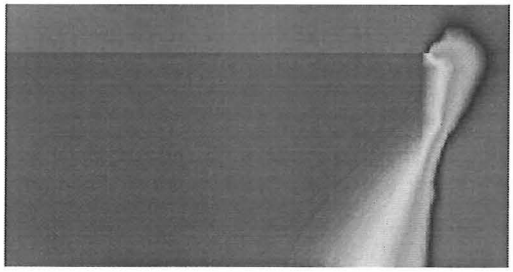

Time = 0.25 second

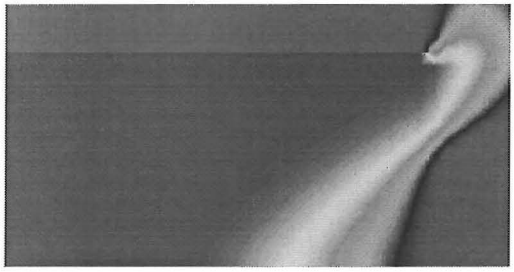

Time = 0.5 second

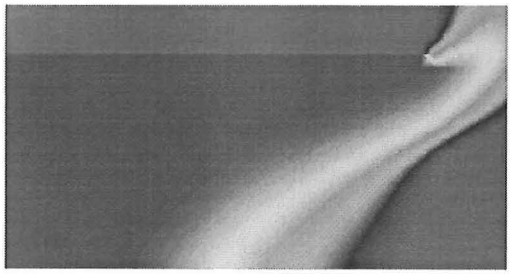

Time = 0.75 second

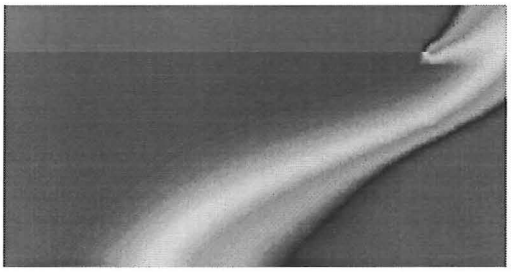

Time = 1.0 second

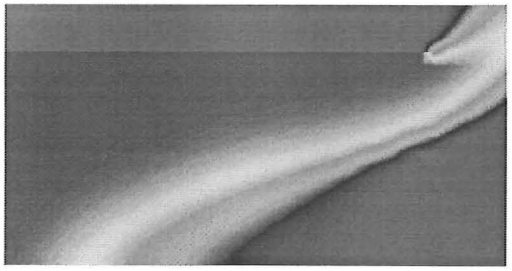

Time = 1.25 seconds

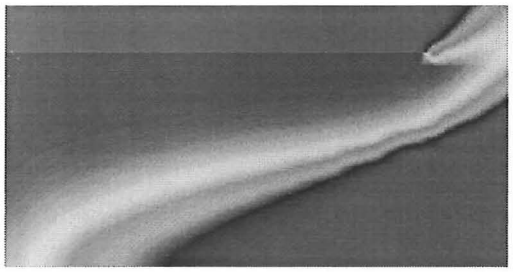

Time = 1.5 seconds

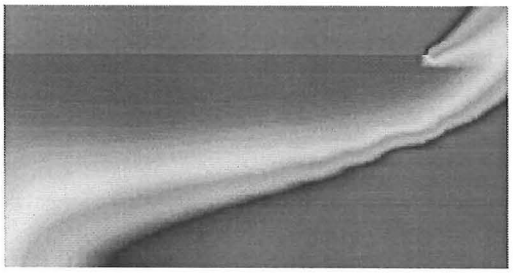

Time = 1.75 seconds

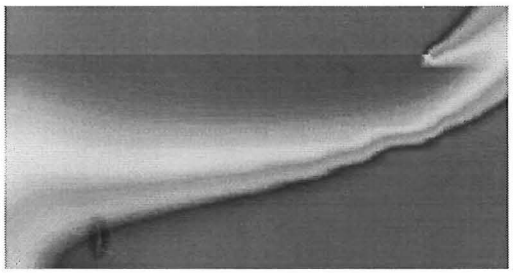

Time 2.0 seconds

salt water density of 1040 kg m^{-3}.

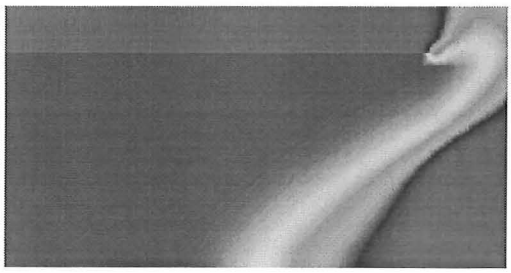

Time = 1.0 second

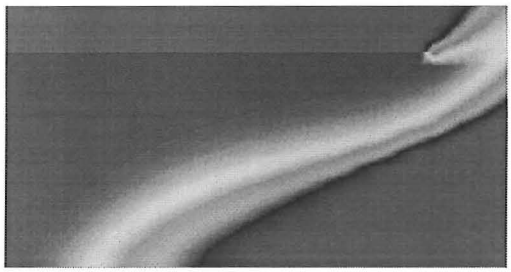

Time = 2 seconds

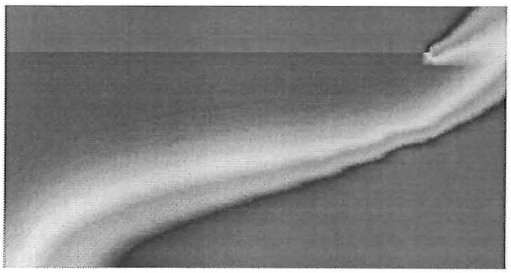

Time = 2.5 seconds

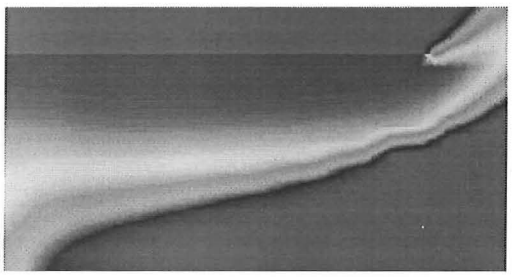

Time = 3.0 seconds

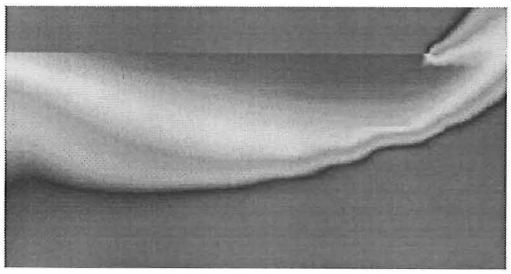

Time = 4.0 seconds

Salt water density of 1010 kg m^{-3}.

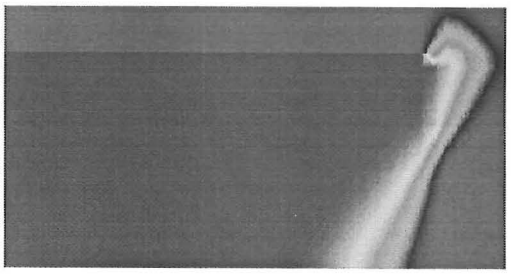

Time = 1.0 second

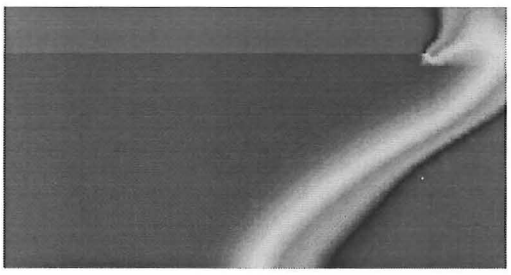

Time = 2.0 seconds

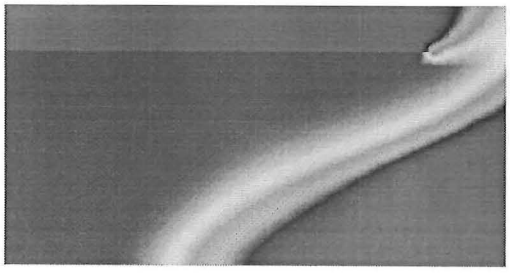

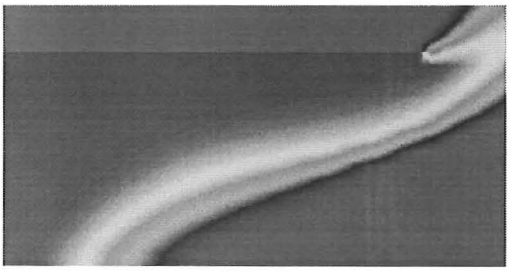

Time = 3.0 seconds

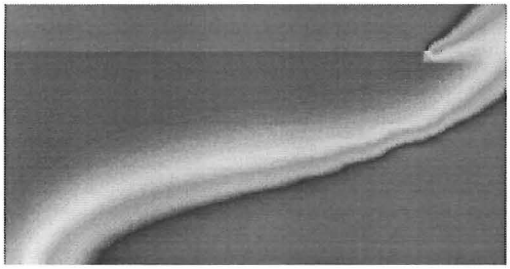

Time = 4.0 seconds

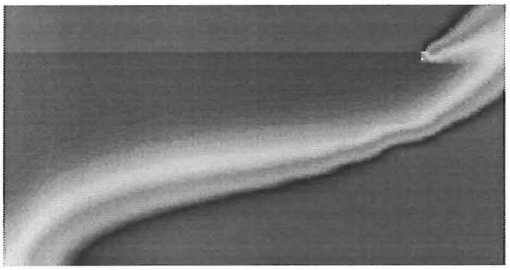

Time = 4.75 seconds

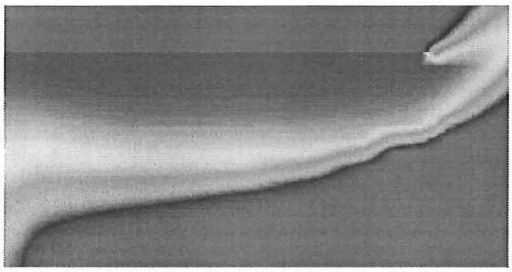

Time = 5.0 seconds

Time = 6.0 seconds

FIRE ENGINEERING RESEARCH REPORTS

95/1	Full Residential Scale Backdraft	I. B. Bolliger
95/2	A Study of Full Scale Room Fire Experiments	P. A. Enright
95/3	Design of Load-bearing Light Steel Frame Walls for Fire Resistance	J. T. Gerlich
95/4	Full Scale Limited Ventilation Fire Experiments	D. J. Millar
95/5	An Analysis of Domestic Sprinkler Systems for Use in New Zealand	F. Rahmanian
96/1	The Influence of Non-Uniform Electric Fields on Combustion Processes	M. A. Belsham
96/2	Mixing in Fire Induced Doorway Flows	J. M. Clements
96/3	Fire Design of Single Storey Industrial Buildings	B. W. Cosgrove
96/4	Modelling Smoke Flow Using Computational Fluid Dynamics	T. N. Kardos
96/5	Under-Ventilated Compartment Fires - A Precursor to Smoke Explosions	A. R. Parkes
96/6	An Investigation of the Effects of Sprinklers on Compartment Fires	M. W. Radford
97/1	Sprinkler Trade Off Clauses in the Approved Documents	G.J. Barnes
97/2	Risk Ranking of Buildings for Life Safety	J.W. Boyes
97/3	Improving the Waking Effectiveness of Fire Alarms in Residential Areas	T. Grace
97/4	Study of Evacuation Movement through Different Building Components	P. Holmberg
97/5	Domestic Fire Hazard in New Zealand	K.D.J. Irwin
97/6	An Appraisal of Existing Room-Corner Fire Models	D.C. Robertson
97/7	Fire Resistance of Light Timber Framed Walls and Floors	G.C. Thomas
97/8	Uncertainty Analysis of Zone Fire Models	A.M. Walker

School of Engineering
University of Canterbury
Private Bag 4800, Christchurch, New Zealand

Phone 643 366-7001
Fax 643 364-2758